SAND2013-1832P

Effect of physical parameter changes on reaction dynamics and stability in gasless reactive multilayer systems

Robert V. Reeves

2011 MRS Fall Meeting
28 November 2011

Sandia National Laboratories is a multi-program laboratory managed and operated by Sandia Corporation, a wholly owned subsidiary of Lockheed Martin Corporation, for the U.S. Department of Energy's National Nuclear Security Administration under contract DE-AC04-94AL85000.

Sandia National Laboratories

Combustion Synthesis of Materials

- Seen as a cost effective method to produce near net size parts from intermetallics, refractories, and ceramics [Holt]
- Can include solid-solid and solid-gas reactions [Holt]
- Can be weakly or strongly exothermic
- Weak systems require preheat – Volume Combustion
- Strong systems exhibit Self-Propagating, High-temperature Synthesis (SHS) [Varma]

Holt, J. B. and Dunmead, S. D., Annual Review of Materials Science 21, 305 1991.

A. Varma; A. S. Rogachev; A. S. Mukasyan; S. Hwang, *Combustion Synthesis of Advanced Materials: Principles and Applications*. Elsevier Science and Technology Books: Amsterdam, 1998; Vol. 24, p 416.

SHS: Basic Process Characteristics

- Ti/2B: T_{ad} = 3190 K, Q = -5.52 kJ/g (-21.61 kJ/cc)
- Al/Co: T_{ad} = 1912 K, Q = -1.28 kJ/g (-6.65 kJ/cc) [Fischer]
- Ni/Ti: T_{ad} = 1583 [Li] K, Q = -0.638 kJ/g (-3.94 kJ/cc) [de Boer]
- To compare, TNT Q = -6.22 kJ/cc [Yaws]
- Propagation rates in mixed powders vary from 0.1 cm/s to 10 cm/s [Varma]
- High heat release and small internal periodicity allows many uses:
  - Small scale devices, e.g. airbag initiators, microthrusters
  - Used for joining, coatings, etc. [Wang]

Fischer, S.H., Grubelich, M.C., SAND98-1176C

B.Y. Li, L.J.Rong, Y.Y.Li, V.E. Gunter, Acta Materialia, Vol. 48, 15, 2000

F.R. de Boer,,R. Boom, W.C.M.Mattens, A.R. Miedema, A.K.Niessen, *Cohesion in Metals Transition Metal Alloys*. North Holland Physics Publishing, Amsterdam; 1989

C. L. Yaws, *Yaws' Handbook of Therm. and Phys.Properties of Chem. Compounds*. Knovel: 2003.

Varma; A. S. Rogachev; A. S. Mukasyan; S. Hwang, *Combustion Synthesis of Advanced Materials: Principles and Applications*. Elsevier Science and Technology Books: 1998; Vol. 24, p 416.

Exothermic Thin Films

- An offshoot from Combustion Synthesis
- High heat release and small internal periodicity allows many uses:
  - Small scale devices, e.g. airbag initiators, microthrusters
  - Used for joining, coatings, etc. [Wang]
- Proposed applications have varied gas environments so understanding effects on reaction behavior is necessary

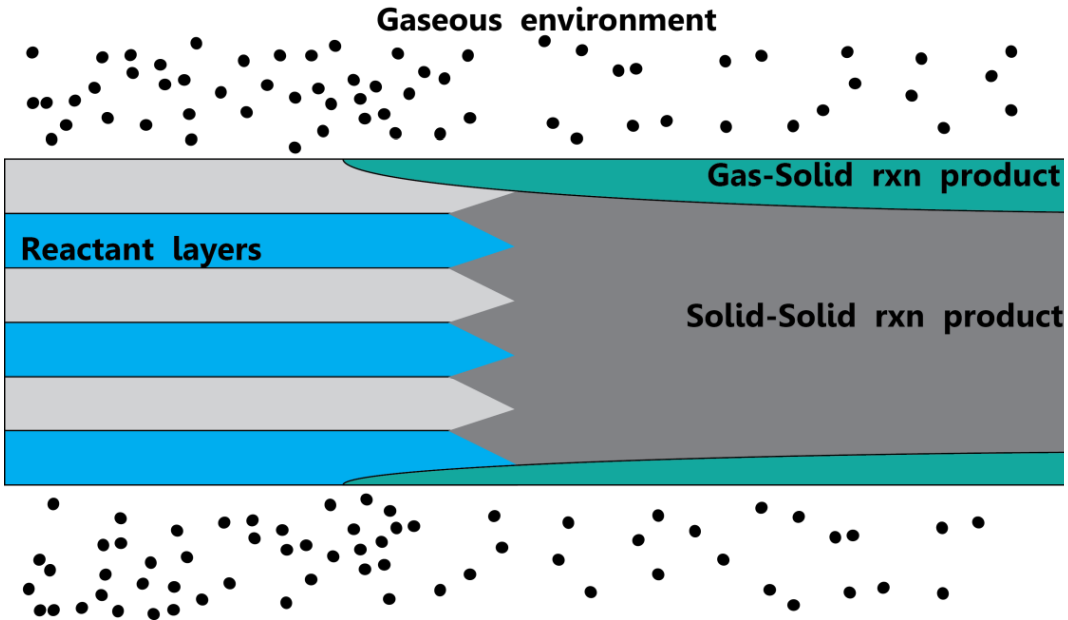

Wang, J., Besnoin, E., Knio, O.M., Weihs, T.P., J. Appl. Phys. 97, 7 2005

SHS: Basic Process Characteristics

- Ti/2B: Q = -122.3 kJ/mol_{atoms} [Fischer]
- Ti/O_2: Q = - 315 kJ/mol_{atoms} [Glassman]
- Multilayered thin films allow precise control of diffusion distances, controlled geometry, and clean interfaces between reactants.
- Propagation rates up to ~90 m/s [Adams]

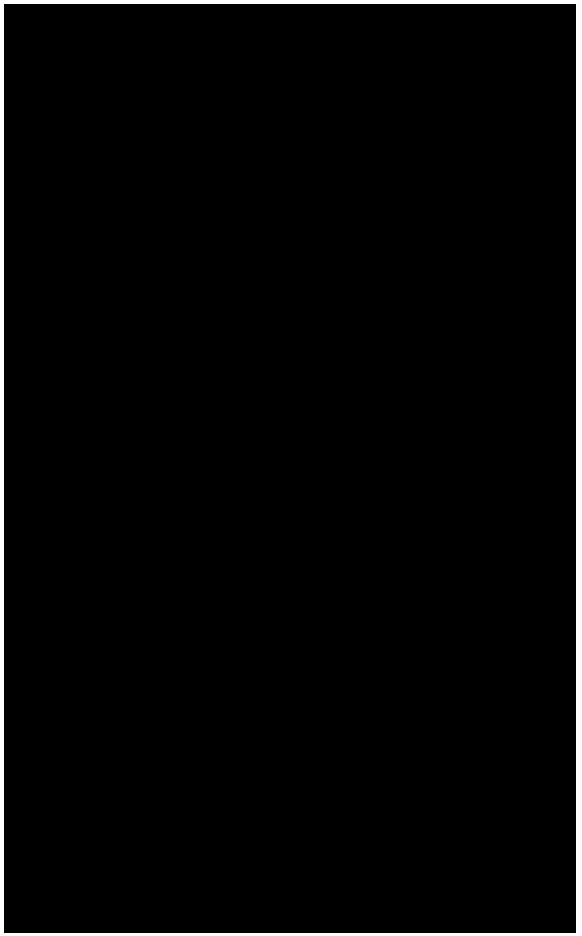

Ti/2B foil, 3.0 μm thick,
300 nm bilayer, @682 Torr

Fischer, S.H., Grubelich, M.C., SAND98-1176C
Glassman, I., *Combustion*. 3rd ed. Academic Press, San Diego, CA: 1996.
Adams, D.P., Rodriguez, M.A., Tigges, C.P., Kotula, P.G., J. Mater. Res., Vol. 21, 12, 2006

Experimental Methods

- Ti/2B films grown by DC planar magnetron sputtering to produce different bilayer thicknesses:
  - 50 nm- to 3000 nm-bilayers, all 3.0 μm thick
- Characterize materials through:
  - Transmission electron microscopy (TEM)
  - X-ray diffraction (XRD)
  - Auger electron spectroscopy (AES)
- Ignite freestanding foils in test chamber
  - Air pressures from ~675 Torr to 10^{-4} Torr
  - Track reaction propagation velocity as function of environmental pressure [O_2 concentration]

Exothermic Thin Films

- Use of multilayered thin films allows for precise control of diffusion distances, controlled geometry, and clean interfaces between reactants.
- Multilayer stacks of nanometric layers of reactive metals
- Bilayer thicknesses in 10's to 100's of nm
- Propagation rates up to ~90 m/s [Adams]

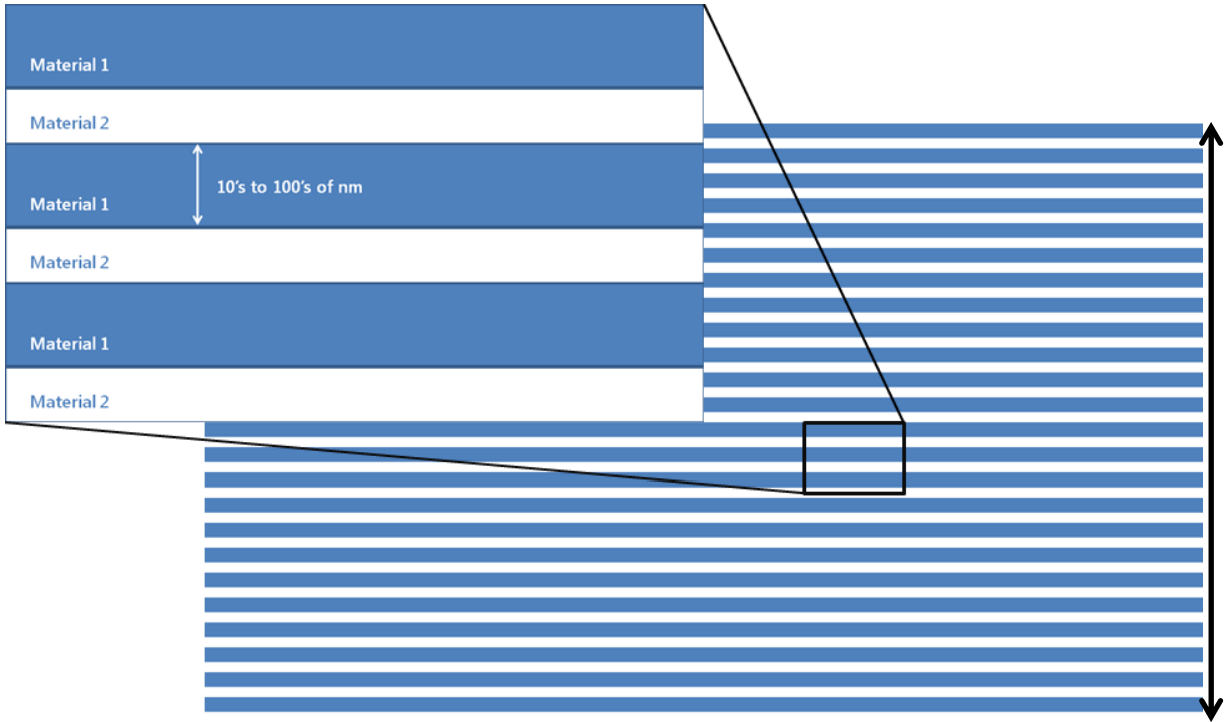

Up to 10's of microns overall thickness

Adams, D.P., Rodriguez, M.A., Tigges, C.P., Kotula, P.G., J. Mater. Res., Vol.

Initial material characterization - X-ray diffraction

- XRD shows only crystalline Ti peaks
  - custom micro-diffractometer system with Rigaku 12 kW rotating anode (Cu)
- B is transparent to these x-rays

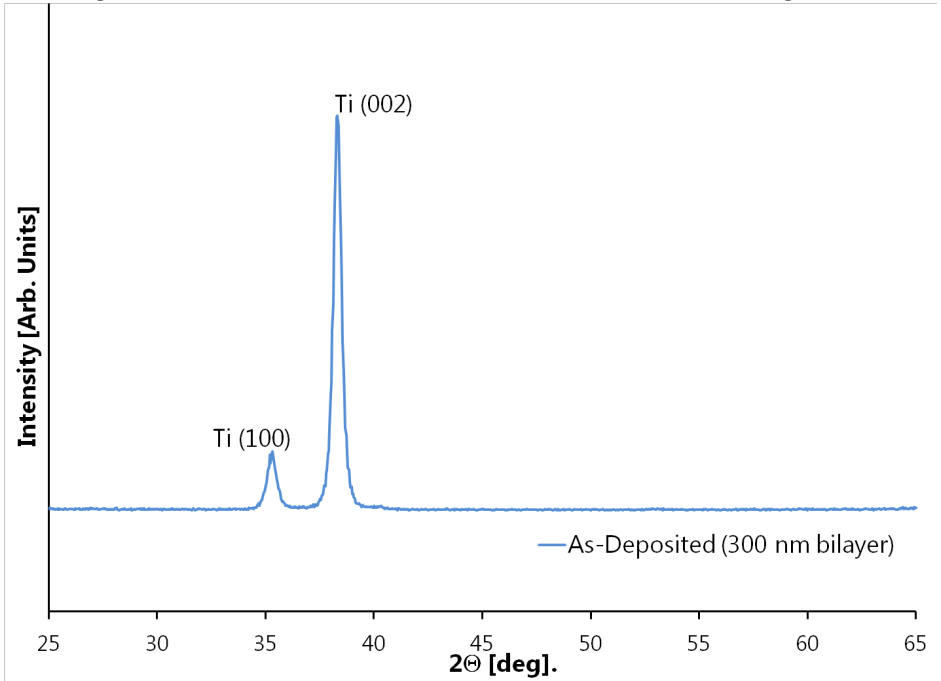

Initial material characterization - Cross Section TEM

- Deposition creates well-ordered multilayer with some roughness between nanocrystalline Ti and amorphous B
  - FFT of B region shows amorphous halos
- Thin region at Ti/B interface contains premixed material or out of plane roughness

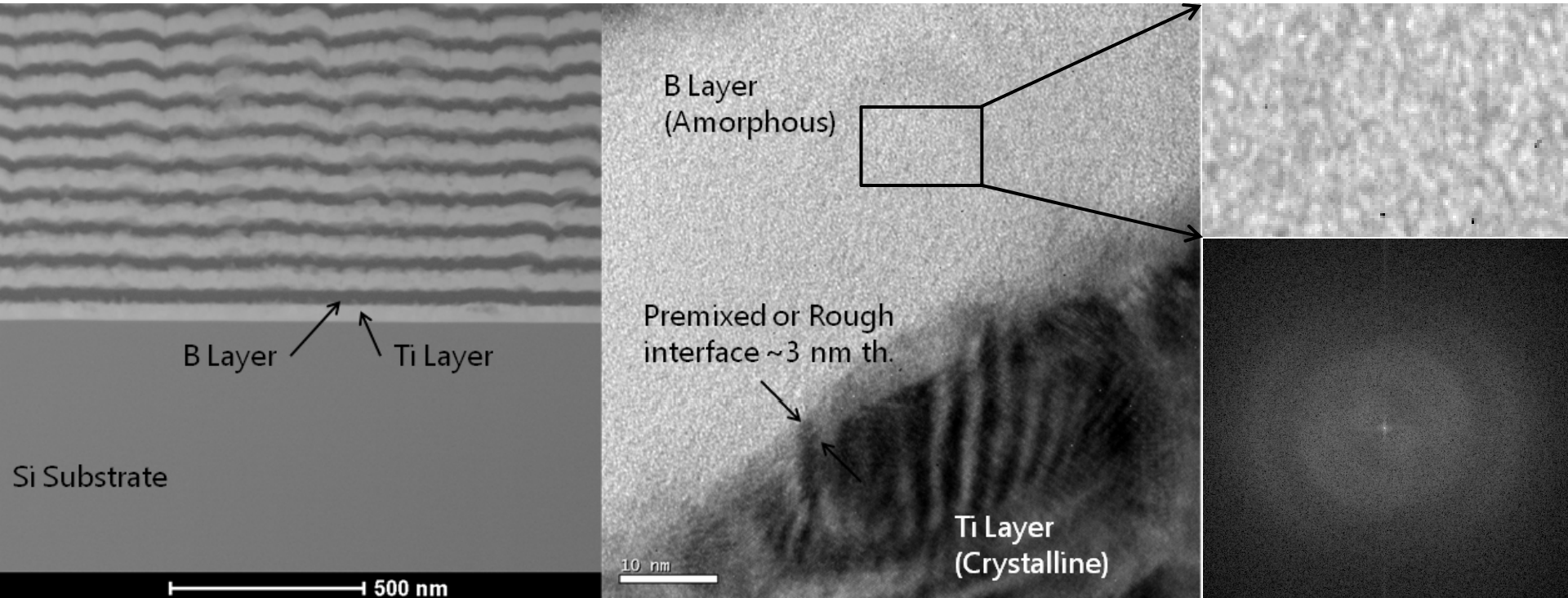

Reaction Propagation Velocity

- Ti/2B foil supported by Kapton tape attached to glass slide
- Commercial Ni/Al reactive foil contacts an edge of the foil
- Ni/Al foil is ignited by capacitive discharge unit
- Heat from Ni/Al autowave ignites Ti/2B foil without excessive preheating
- Vacuum level of chamber controlled – gas is residual air

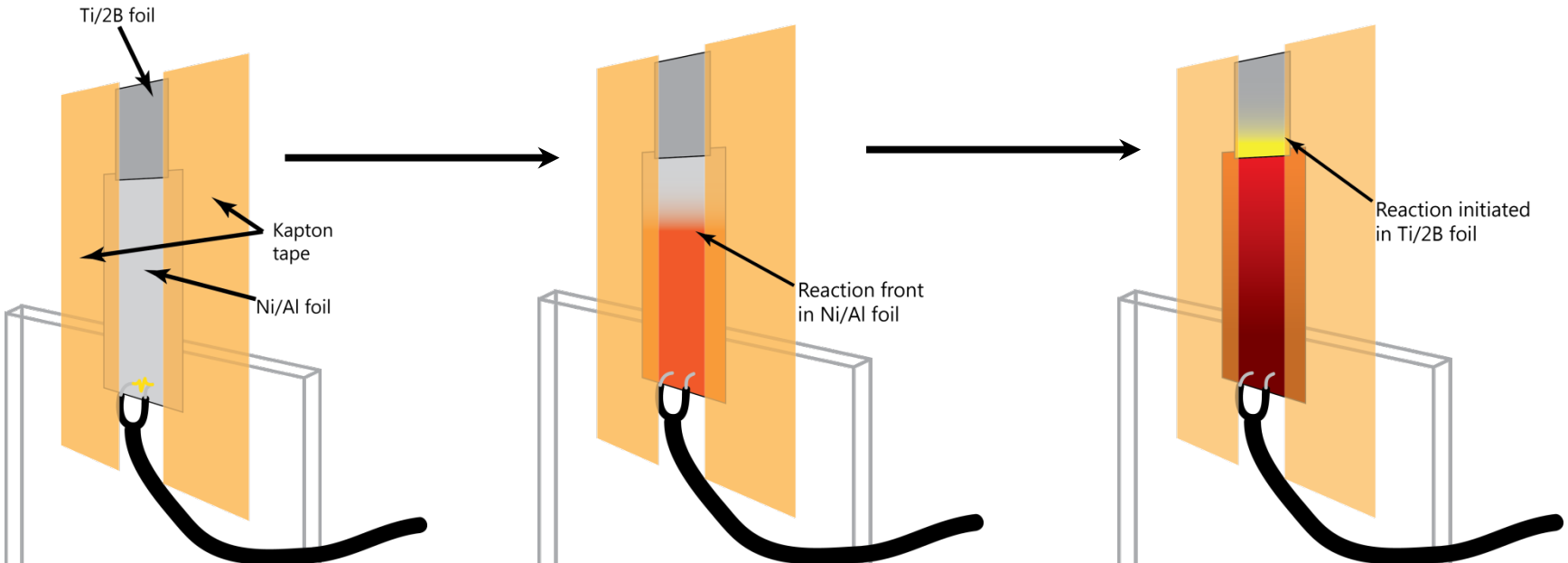

Pressure dependence as a function of bilayer

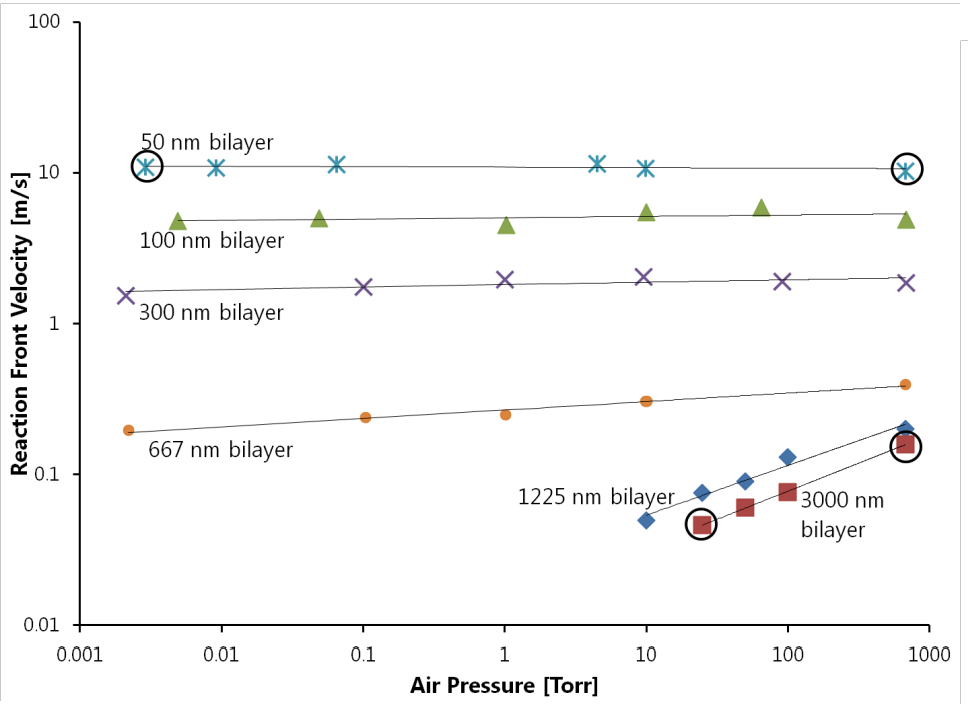

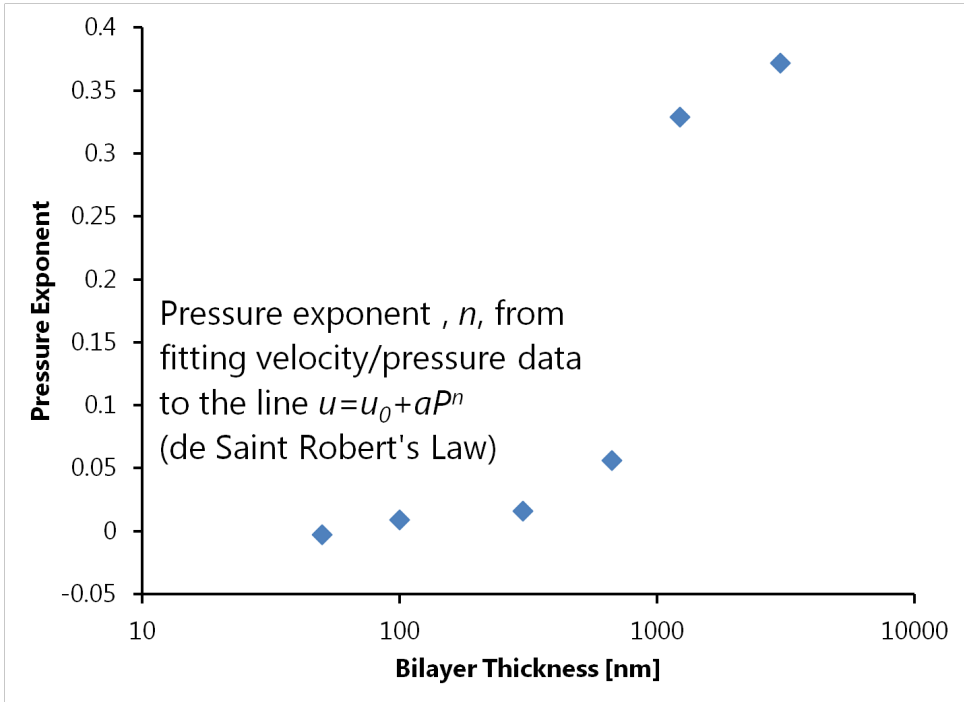

- Thick bilayers (1225& 3000 nm) have strong dependence on air pressure
- Thin bilayers (≤667 nm) have little dependence on air pressure
- Transitional bilayer thickness between 667 and 1225 nm

Velocity comparison:
50 nm bilayer vs 3000 nm bilayer

1 s real time = 500 μs elapsed reaction time (total elapsed time is 39 ms)

Wave front comparison

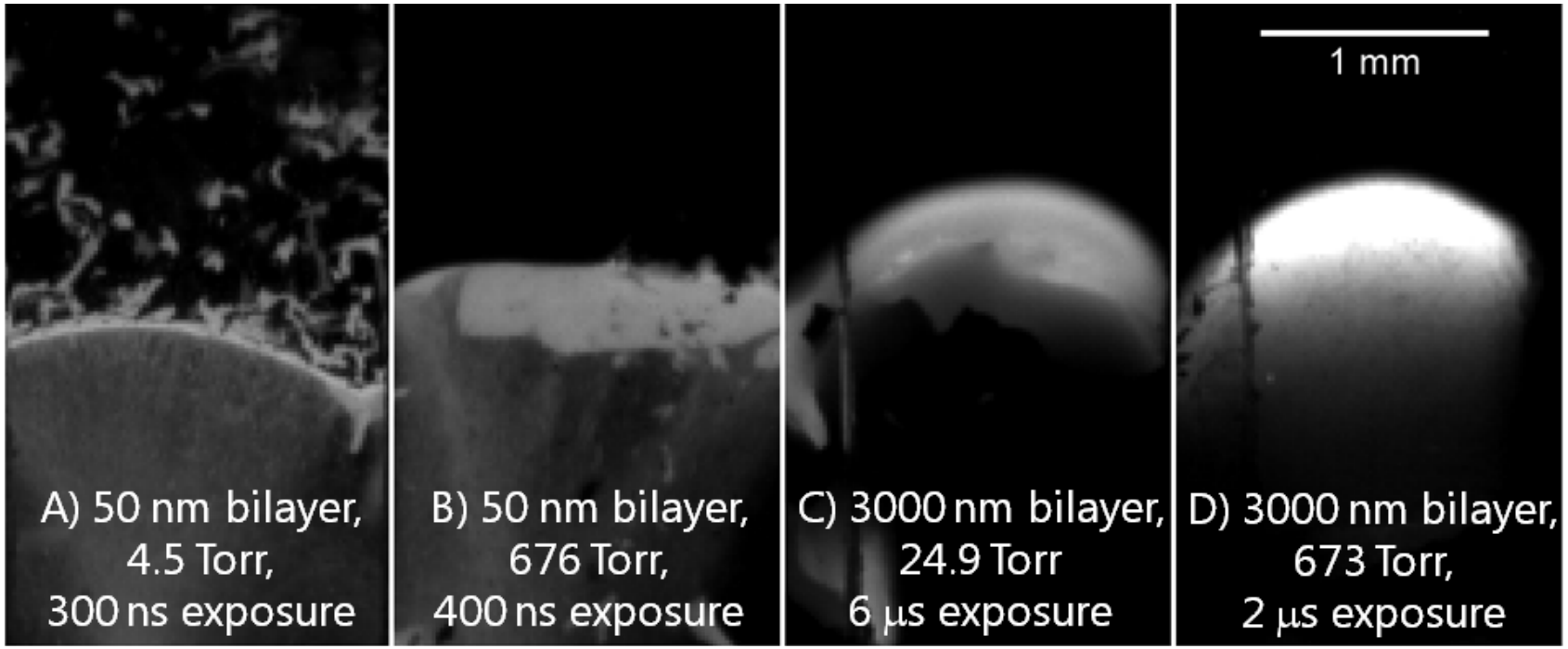

- Luminosity nearly constant for 50 nm bilayer foil across all pressures
- 3000 nm foil decreases in luminosity >6x between 670 and 25 Torr
- Reaction front thin in 50 nm foil, typical thin front for high activation energy, fast kinetics like nanometrically mixed condensed phase reaction
- Broad front in 3000 nm foil, typical for low activation energy, slow kinetics gas-solid diffusion reaction

Velocity vs Bilayer at different pressures

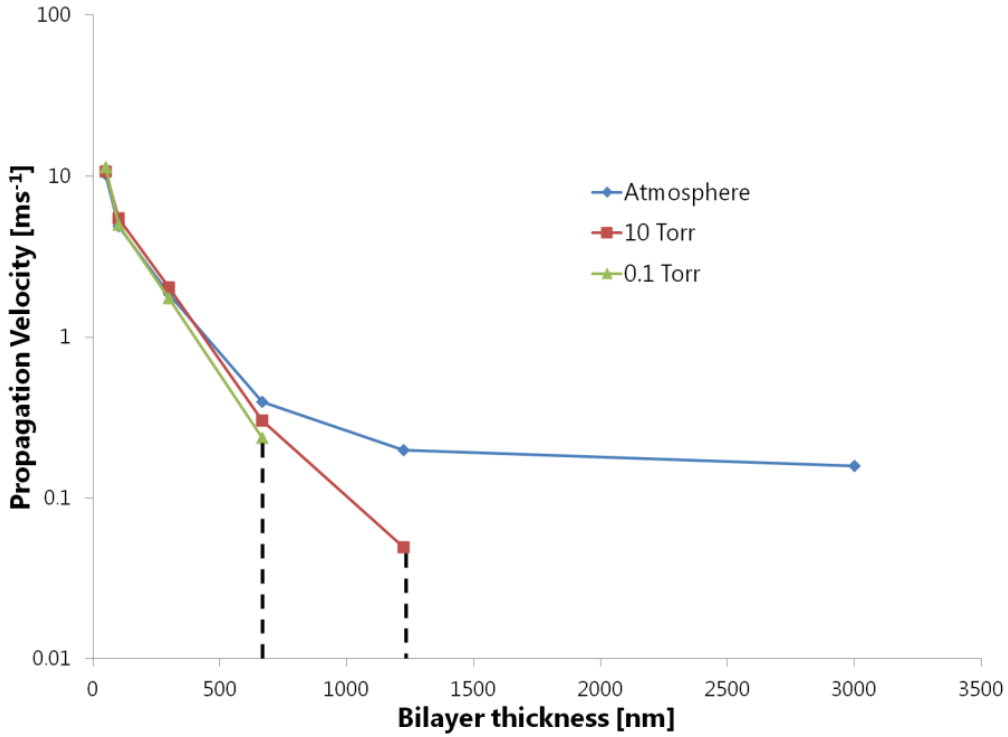

- Velocity/bilayer curves have different trends at different pressures
- Deviation from atmosphere occurs at 667 nm bilayer thickness

Chemical phases by XRD analysis – Reacted at atmospheric pressure

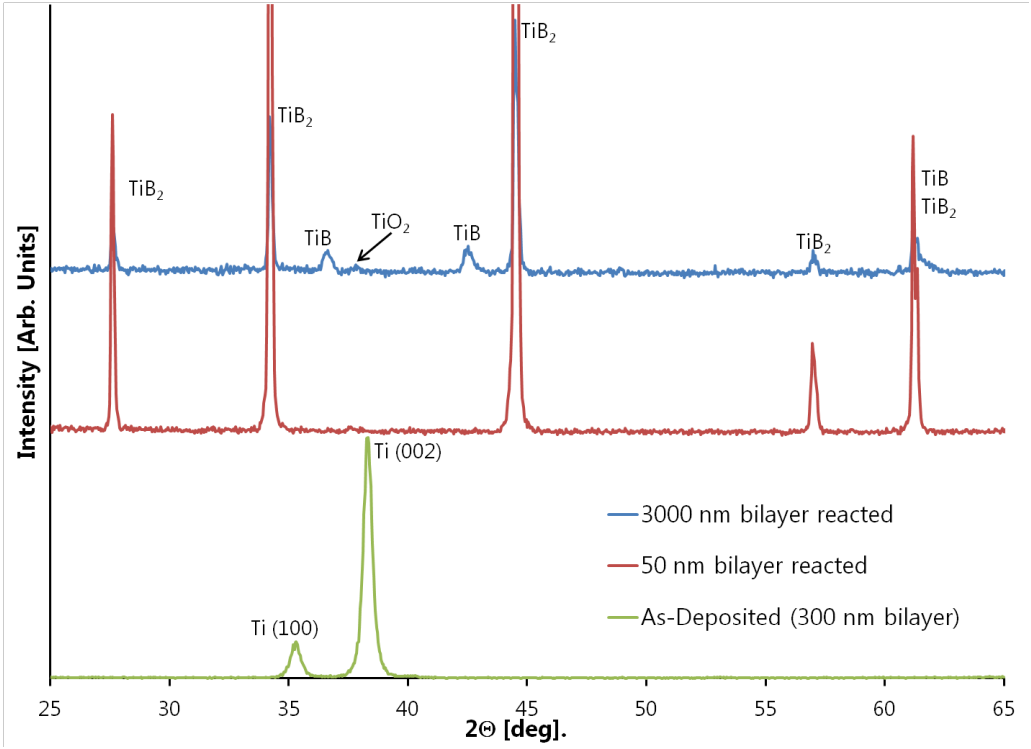

- Only TiB_2 phase formed in 50 nm bilayer foils
- 3000 nm bilayer foil has trace TiO_2, TiB, and TiB_2
  - Formation of TiO_2 could be underestimated due to flaking, prevalence of amorphous structure

Auger electron spectroscopy – 3000 nm bilayer foil at 670 Torr

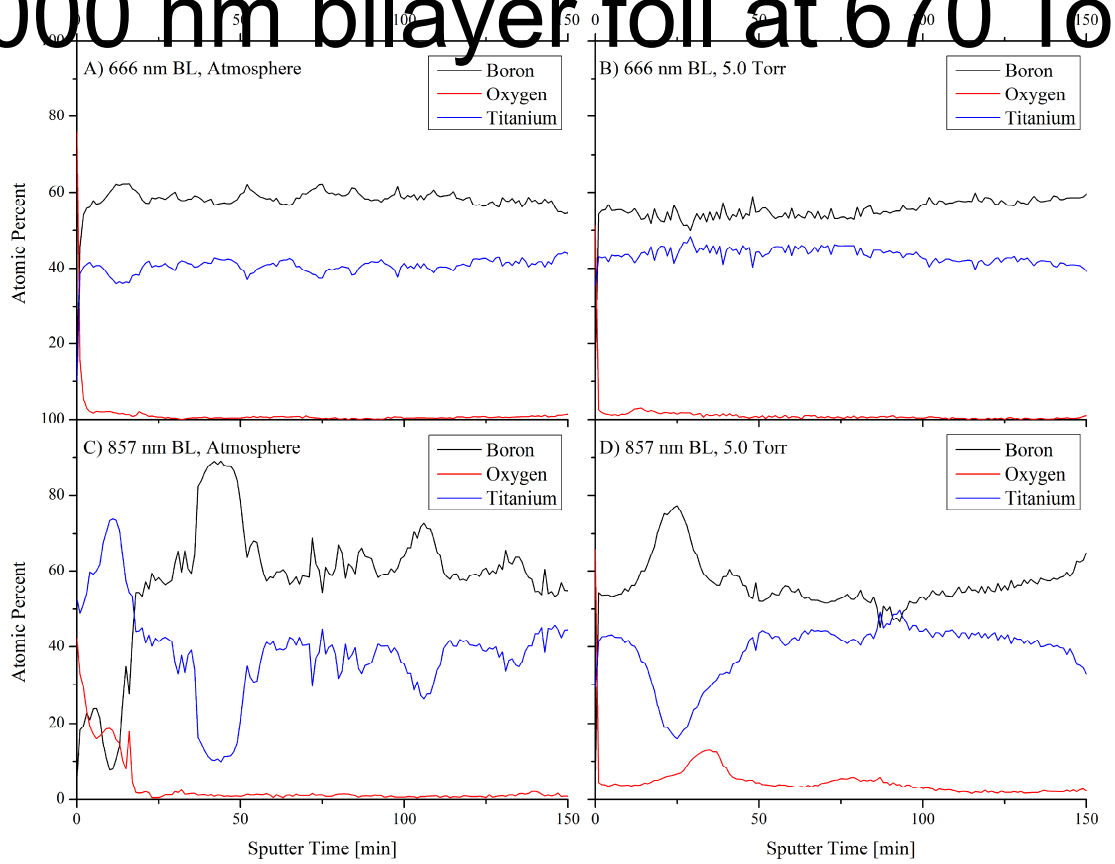

- Significant oxygen concentration at outer surface, decreases with increasing depth and increasing B concentration
- Region with Ti:B ratio of ~1:2 – responsible for TiB2 crystal peaks.
- Large region of unreacted B – B diffusing into Ti, but reaction incomplete

Conclusions

- Growth of Ti/2B films with DC biased sputtering produces well-controlled multilayers with little premixing of reactants
- Thin bilayers (≤667 nm) have little air pressure dependence, so solid-solid reaction of $Ti+2B \rightarrow TiB_2$ dominates
- Thick bilayers (<667 nm) have increasing and large pressure dependence as well as defined quenching pressures, so gas-solid $Ti+O_2 \rightarrow TiO_2$ is important
  - Heat release likely drives subsequent $Ti+2B \rightarrow TiB_2$ reaction
  - Decreasing pressure exponent with decreasing bilayer thickness indicates $Ti+2B \rightarrow TiB_2$ heat release rate increases in importance

XRD: Ni/Ti 6.25 nm bilayer, 5 μm thick - Joel McDonald

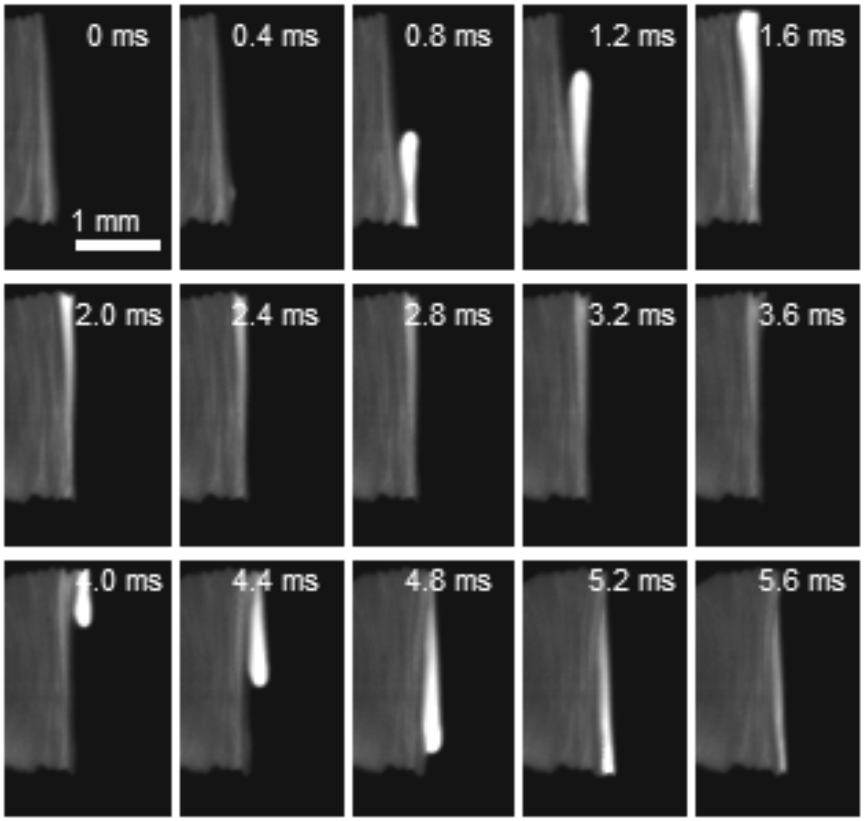

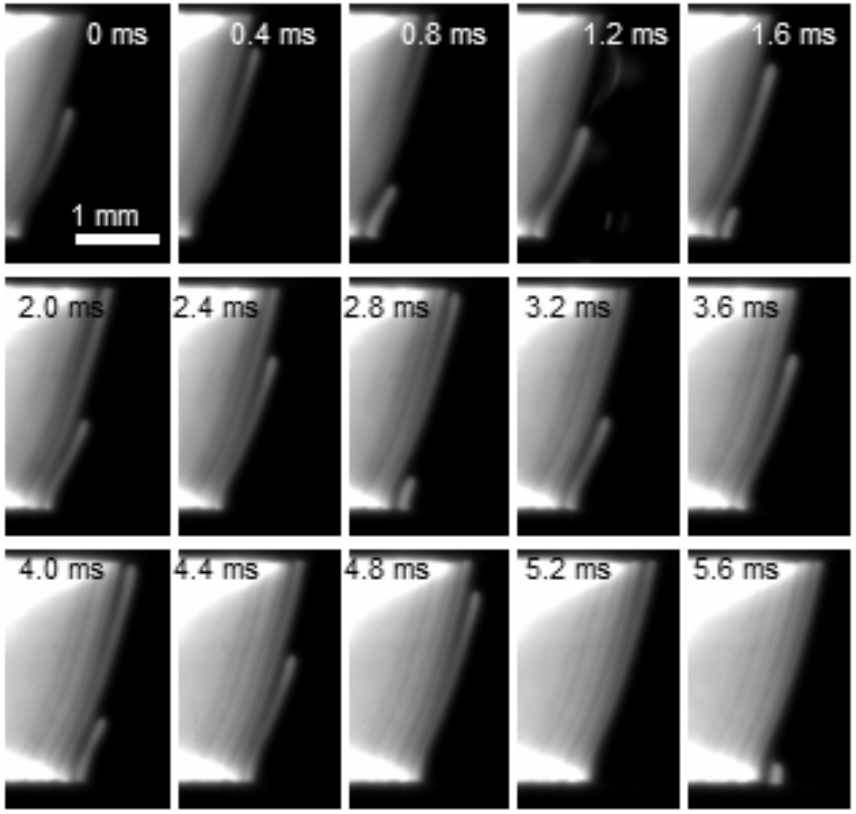

- Reaction at 300 mTorr
- Spin wave of intermetallic reaction only mode present

- Reaction at atm. pressure
- Spin wave followed by bright combustion wave

XRD: Ni/Ti 5 μm thick

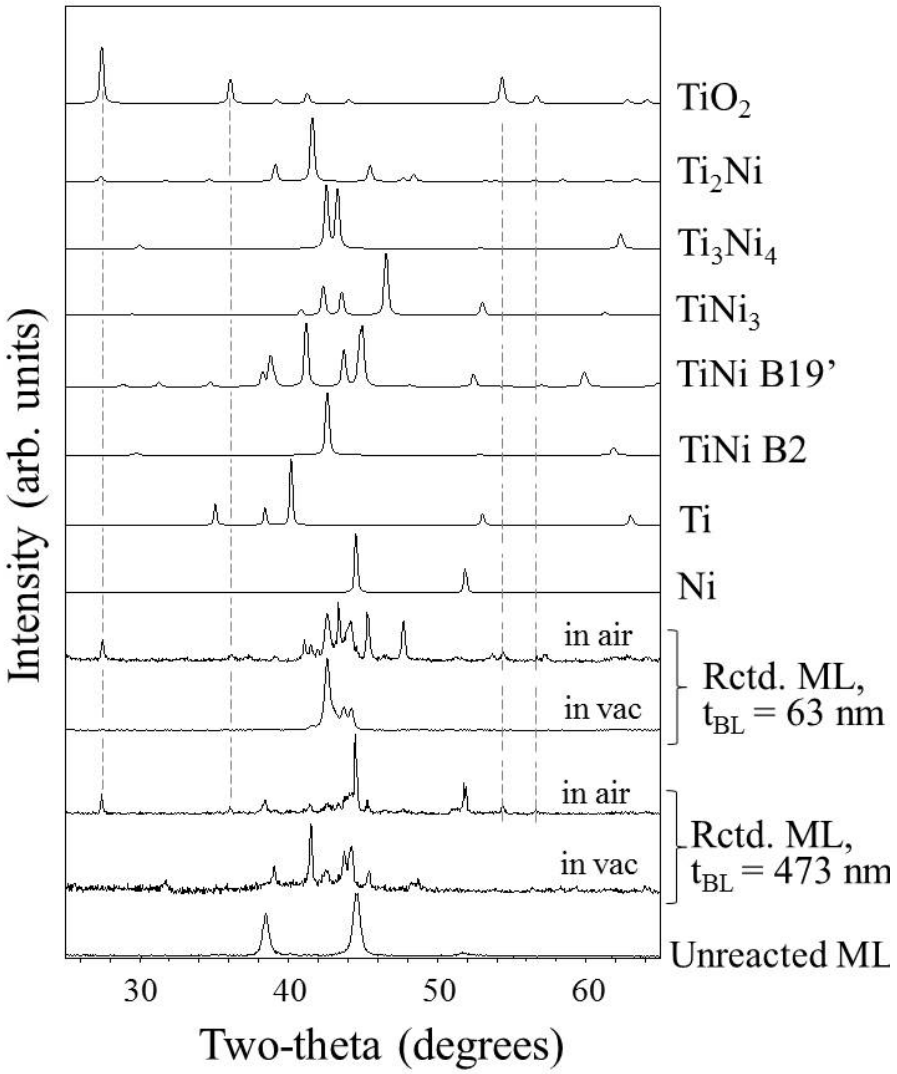

- Chemical phases formed during reaction in air compared to reaction in vacuum
- Foil reacted at 1mTorr exhibits only Ni+Ti phases
- Reaction in air produces Ni+Ti phases plus Ni and Ti oxides

Auger: Ni/Ti 5 μm thick

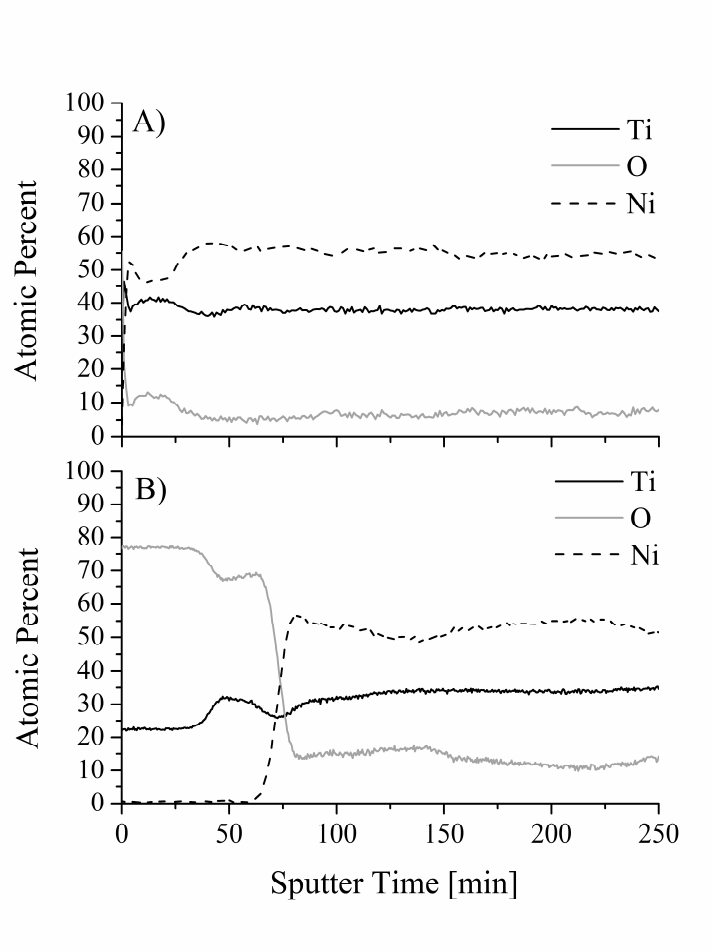

- AES shows thick O penetrated, Ti rich layer for 473 nm BL foils in air
- Little O penetration at 1 mTorr
- Excess Ni in interior

Reaction velocity as function of pressure: Ni/Ti 473 nm bilayer, 5 μm thick

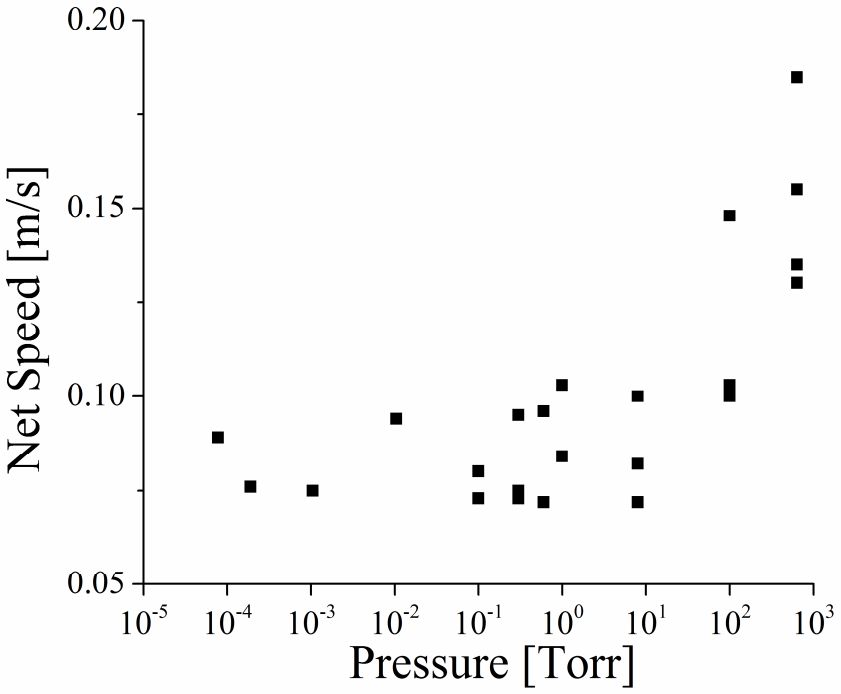

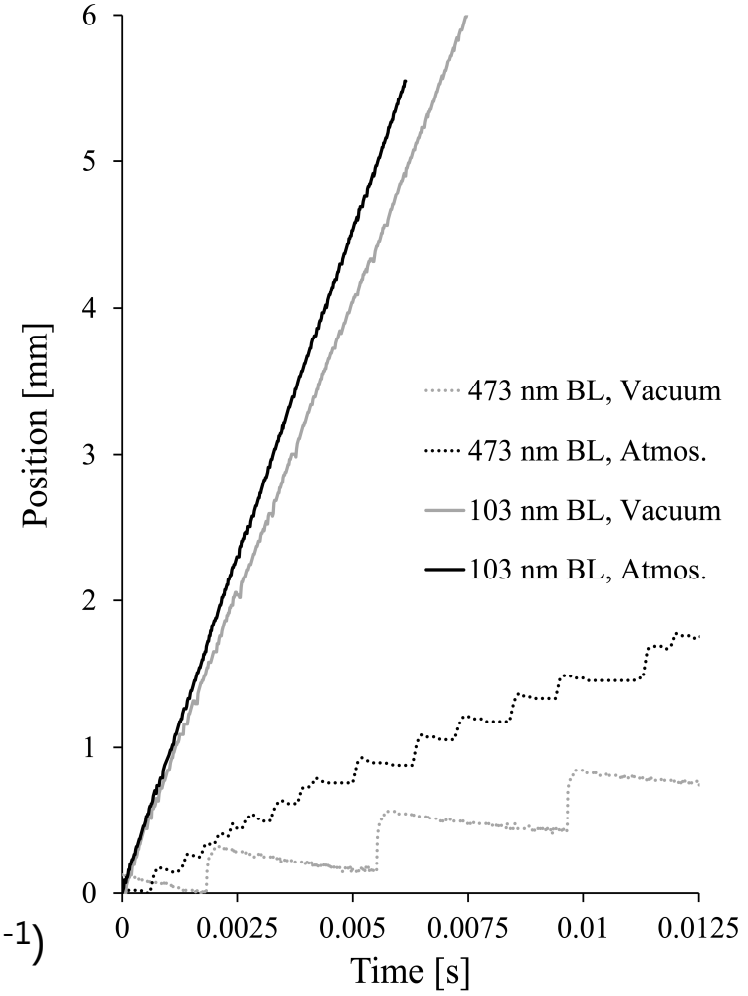

- Reaction velocity increases with air pressure
- Avg. transverse band width increases ~3x at decreased pressure
- Nucleation rate is vastly decreased (180 s^{-1}>>800 s^{-1})

Summary – Ni/Ti Thin Films

- Ni/Ti films propagate with unstable, spinning reaction fronts
- Spin occurs over wide bilayer design and in investigated vacuum range
- Air pressure decreases transverse band width and increases frequency
  - Adds stability to reaction front
  - Begins to approximate steady reaction front
- Heat release from Ti oxidation increases forward heat transfer

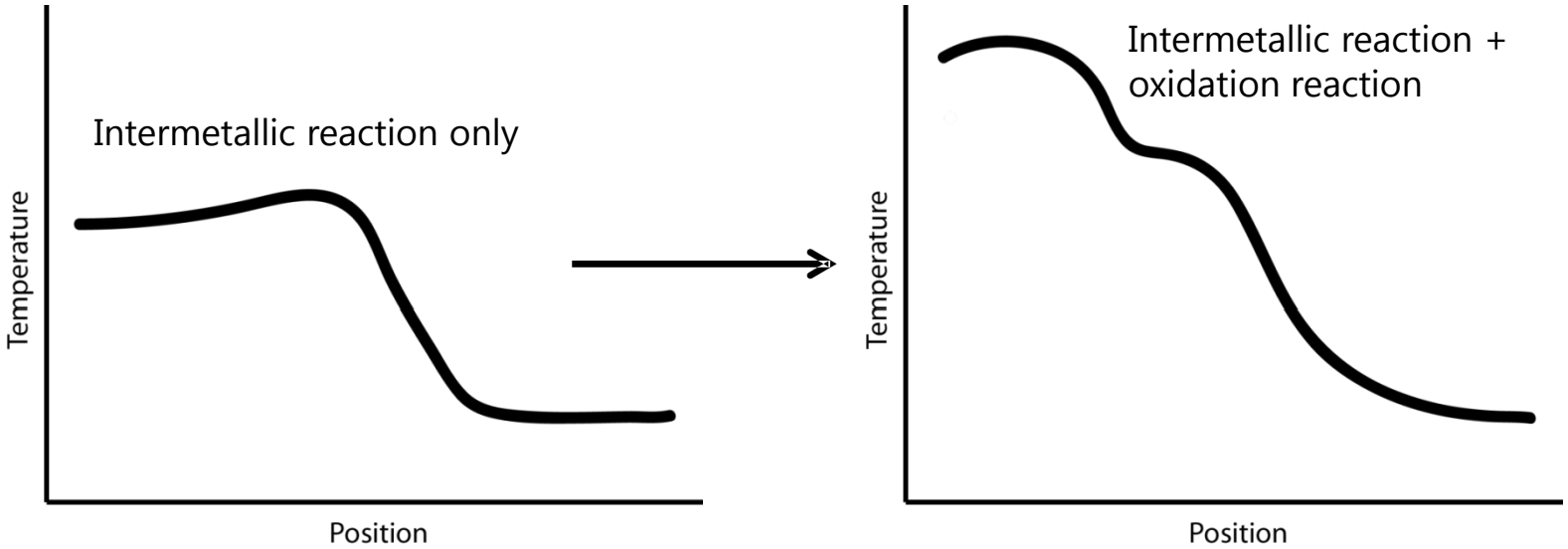

SHS: Basic Process Characteristics

- Ti/2B: Q = -122.3 kJ/mol_{atoms} [Fischer]
- Ti/O_2: Q = - 315 kJ/mol_{atoms} [Glassman]
- Proposed applications have varied gas environments so understanding effects on reaction behavior is necessary

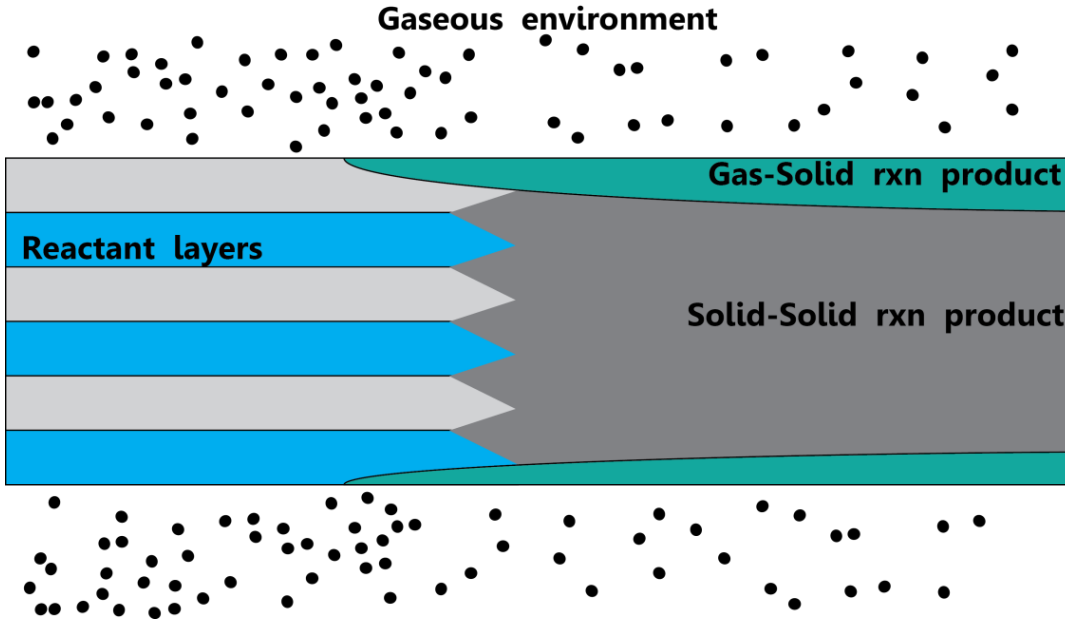

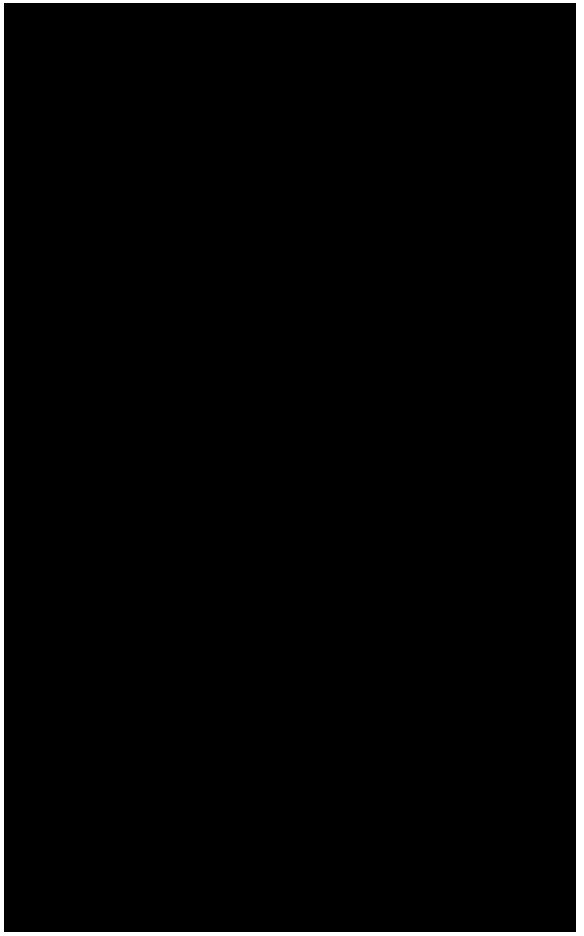

Ti/2B foil, 3.0 μm thick,
300 nm bilayer, @682 Torr

Fischer, S.H., Grubelich, M.C., SAND98-1176C
Glassman, I., *Combustion*. 3rd ed. Academic Press, San Diego, CA: 1996.

RVR6

Co/Al Exothermic Foils and Spin

- In large foil, ignition creates preheated zone (center)
- Separate spin waves are emitted from preheated zone and wrap around ignition zone and each other
- In small foil ignited on end, spin wave looked like stacked transverse bands
- A sign of instability in reaction, prior to quenching

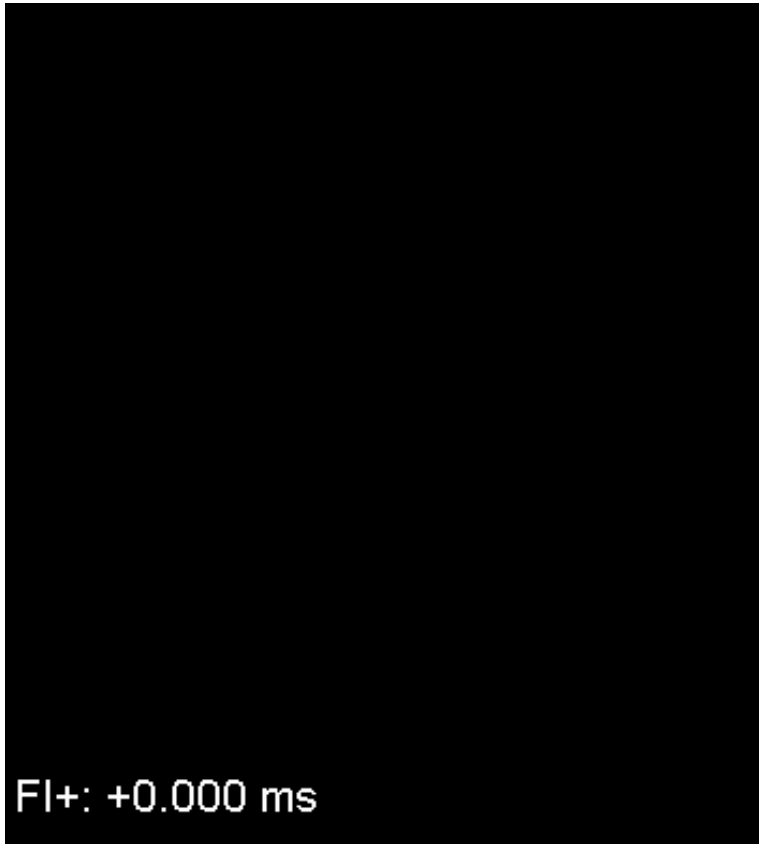

RVR6 Needs
Movie or images of spin
plot of vel. vs. bilayer
rvreeve, 9/23/2011

Experimental Methods

- Films grown by DC planar magnetron sputtering to produce different bilayer thicknesses:
- Characterize materials through:
  - Differential Scanning Calorimetry (DSC)
  - Transmission electron microscopy (TEM)
  - X-ray diffraction (XRD)
  - Auger electron spectroscopy (AES)
- Ignite freestanding foils in test chamber
  - Air pressures from ~675 Torr to 10^{-4} Torr
  - Track reaction propagation velocity as function of environmental pressure [O_2 concentration]

RVR7

Differential Scanning Calorimetry of Reactive Foils

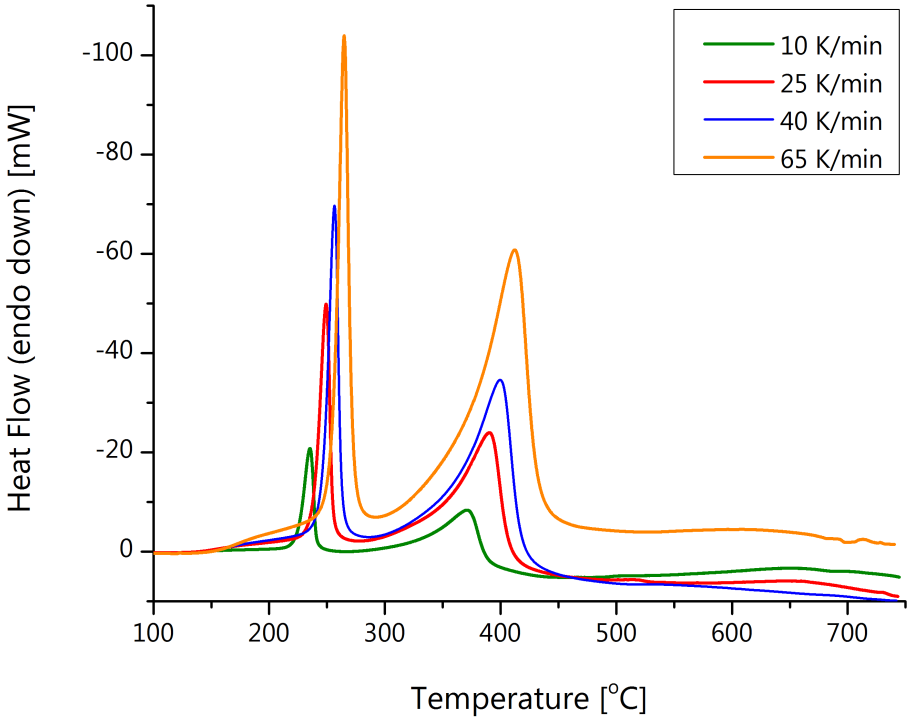

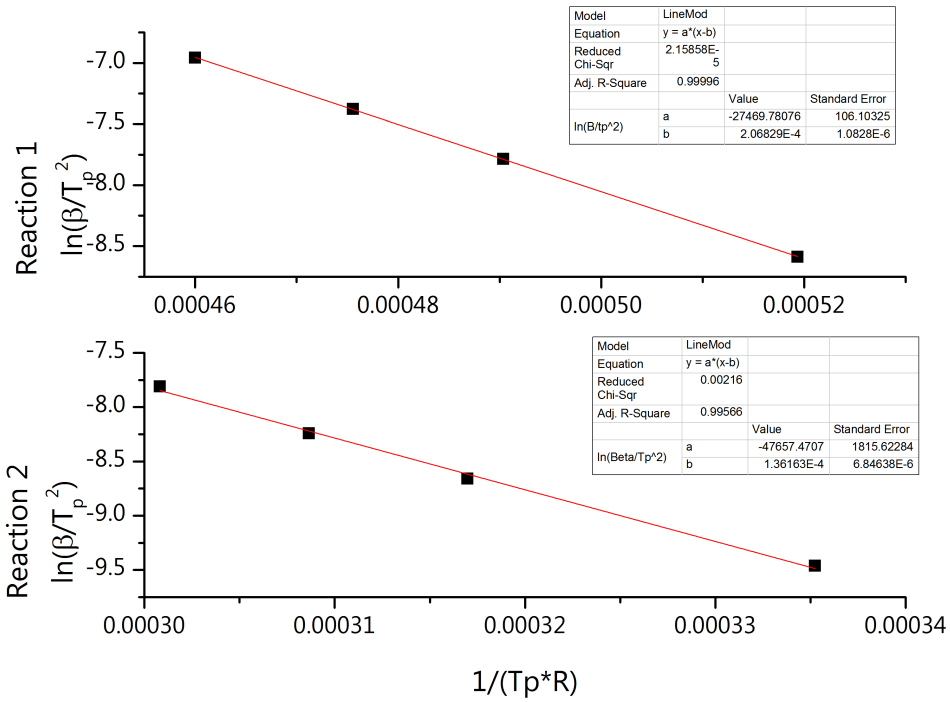

Co/Al foil 21 nm bilayer

- Only exhibits 2 exotherms
- Exotherms at same onset temperature as in 66.4 nm design
- Does not exhibit spin in SHS mode

Slide 26

RVR7 Figures for heat release for each material

rvreeve, 9/23/2011

RVR8

DSC of Co/Al Reactive Foils – Phase ID

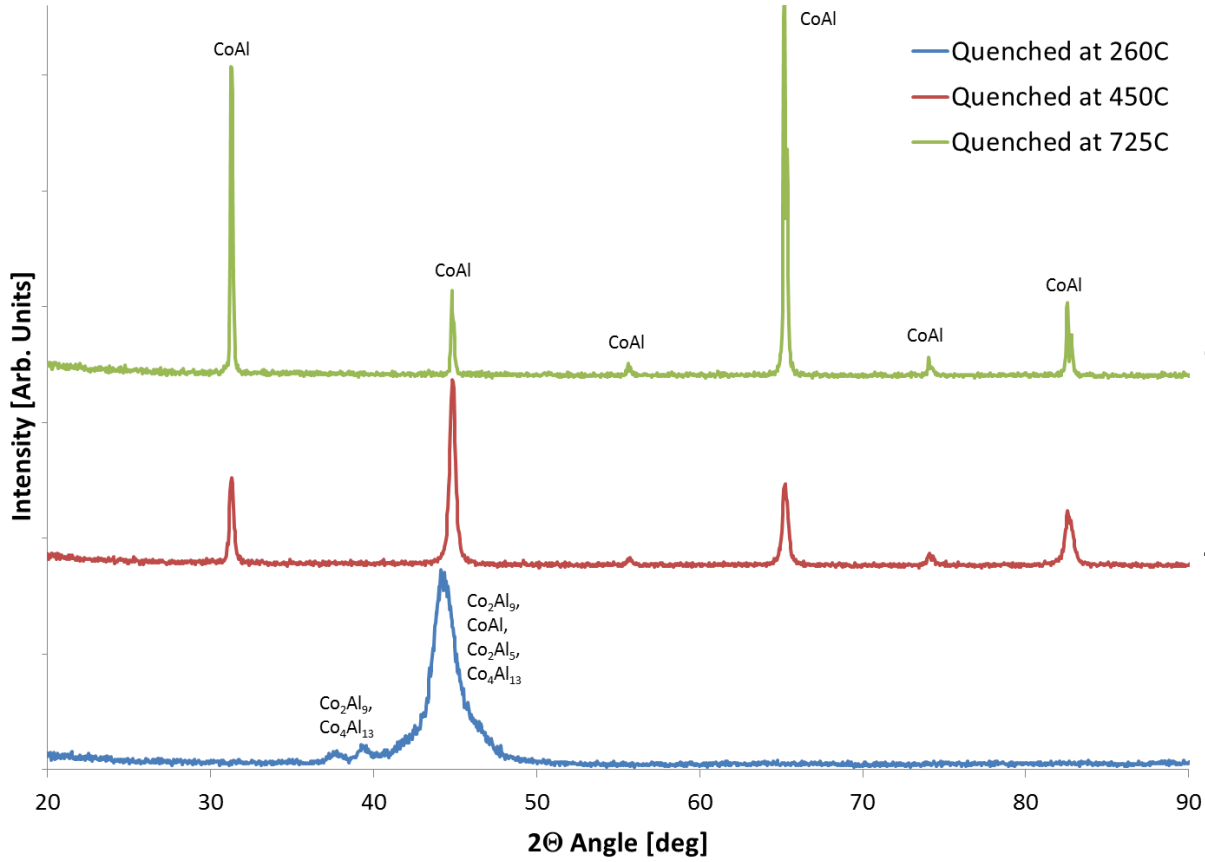

3: Ea not quantifiable

2: Ea= 47658±1816 kJ/mol

1: Ea= 27470±106 kJ/mol

- 1. Al is fully integrated into products, including off-stoichiometry products
- 2. Products form final CoAl product phase:
- 3. Texturing and grain growth of CoAl – Too gradual for calculation of apparent Ea with DSC

Slide 27

RVR8 Figures for heat release for each material

rvreeve, 9/23/2011

RVR9

Differential Scanning Calorimetry of Reactive Foils

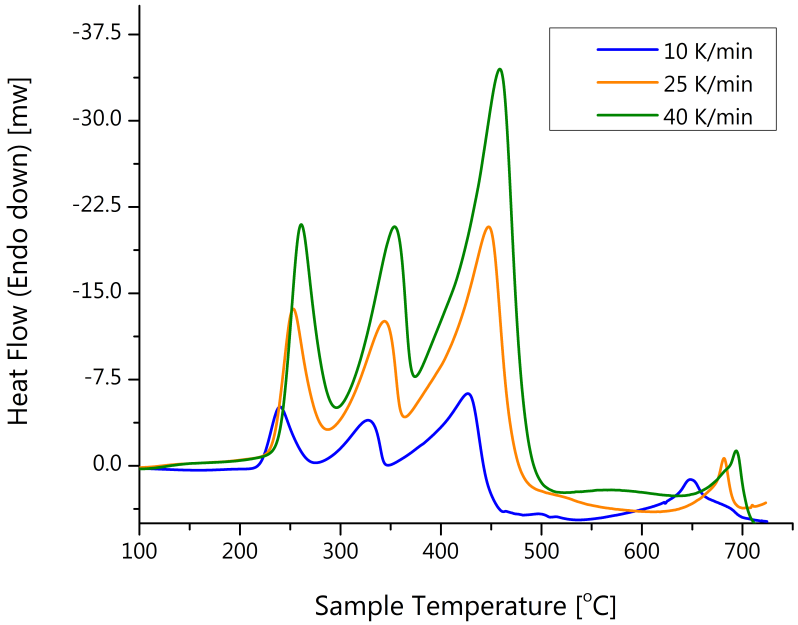

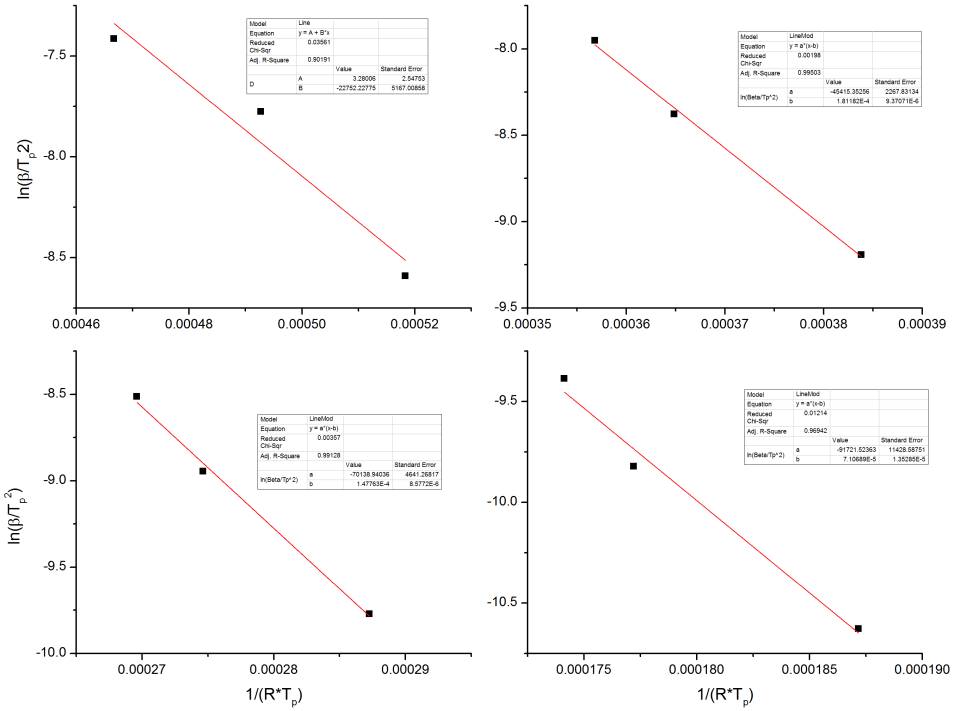

Co/Al foil 66.4 nm bilayer
-4 distinct exotherms
-Exhibits spin in SHS mode

Slide 28

RVR9 Figures for heat release for each material

rvreeve, 9/23/2011

RVR10

DSC of Co/Al Reactive Foils – Phase ID

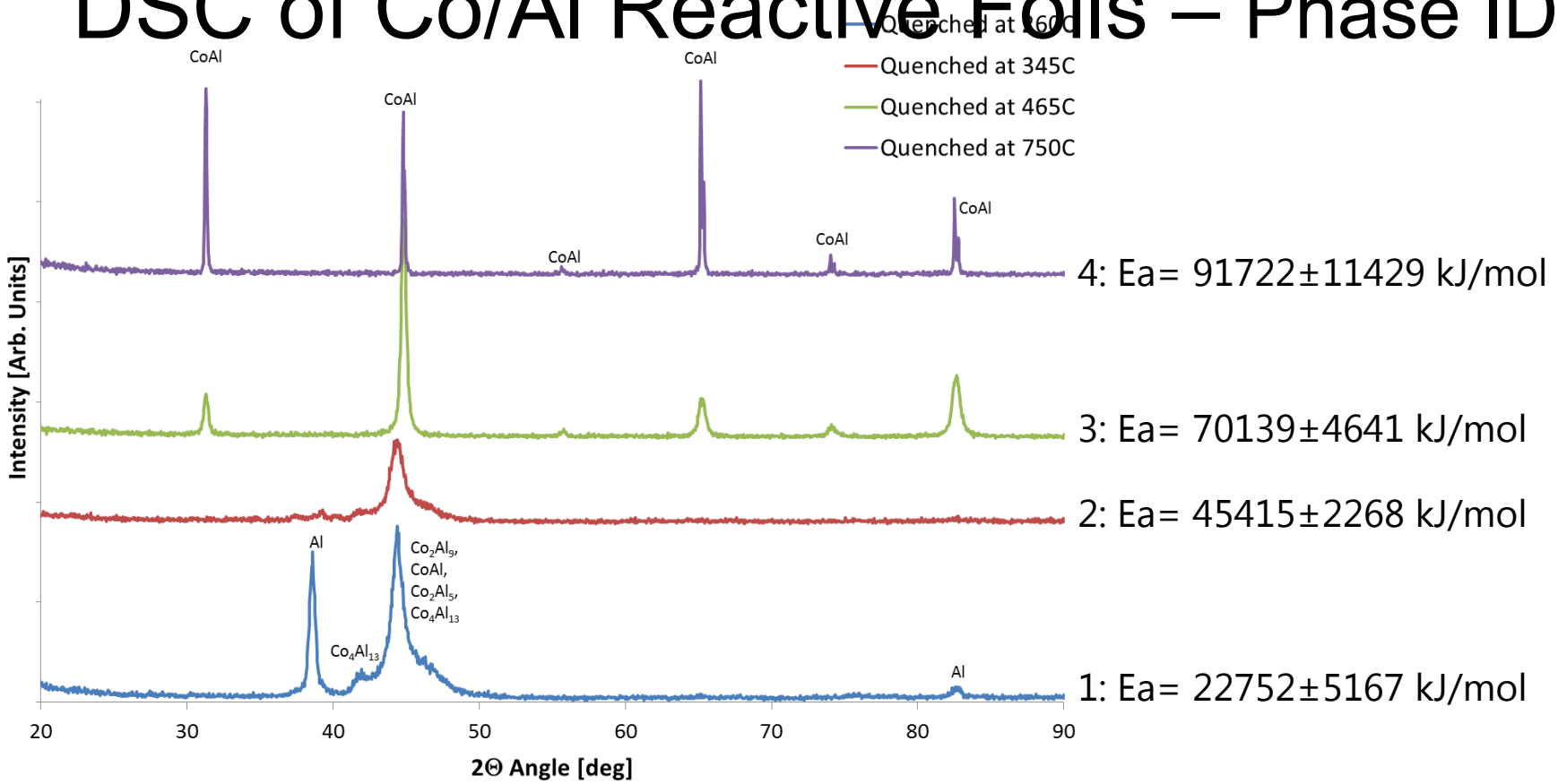

- 1. Initial interfacial reaction produces intermediate aluminides, Co does not fully diffuse into Al
- 2. Al is fully integrated into products, including off-stoichiometry products
- 3. Products form final CoAl product phase:
- 4. Texturing and grain growth of CoAl

Slide 29

RVR10 Figures for heat release for each material
rvreeve, 9/23/2011

Kinetics Results

- Initial reactions have corresponding apparent activation energies despite bilayer thicknesses
  - Interfaces the same despite thicker bilayers
- Much higher apparent Ea for complete conversion to Co/Al at thicker bilayers
  - Likely due to formation of successive diffusion couples at Co/Al interface during reaction

Material	E_{a1} [J/mol]	E_{a2} [J/mol]	E_{a3} [J/mol]	E_{a4} [J/mol]
Co/Al 21 nm bilayer	27470±106	47658±1816	N/A	N/A
Co/Al 66.4 nm bilayer	22752±5167	45415±2268	70139±4641	91722±11429

Reaction Wave Stability

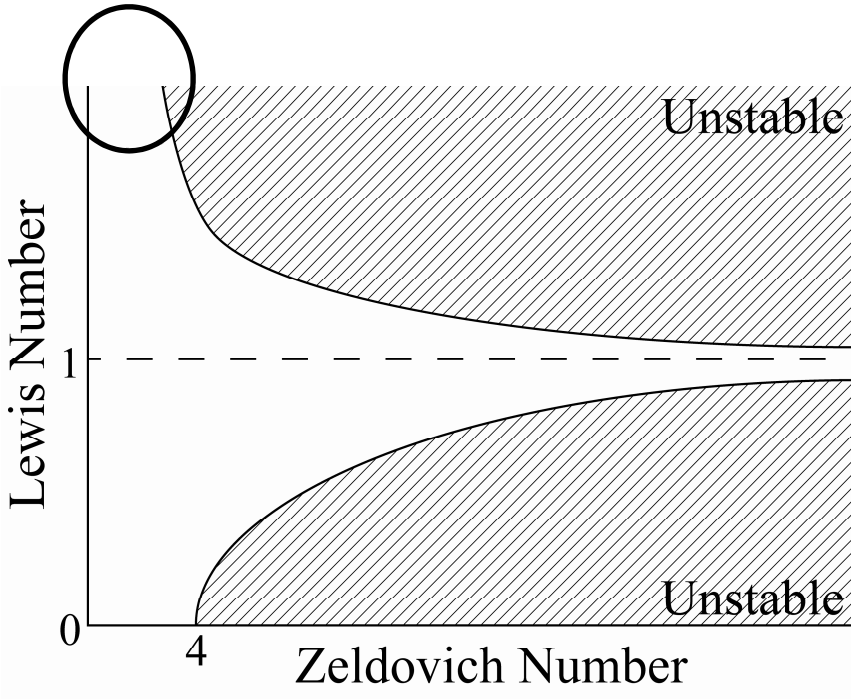

- Above chart from Aldushin and Kasparyan [1,2], discussed by Merzhanov and Rumanov[3]

- Lewis Number, $\frac{\alpha}{D} = \frac{\kappa}{D\rho c}$
  - Compares Mass Diffusion and Thermal Diffusion rates
  - Typical $L_e \approx \frac{10^{-1}}{10^{-3}\ to\ 10^{-7}}$ for gasless systems

- Zel'dovich Number,

$$\beta = \frac{E_a}{RT_{ad}{}^2}(T_{ad} - T_0)$$

  - Compares temperature dependence of reaction to adiabatic flame temp.

[1] *Sov. Phys. Dokl,* **24**, 29, 1979
[2] *Akad. Nauk SSSR*, **247**, 1112, 1979)
[3] *Reviews of Modern Physics*, **71**, 4, 1999

Effect of Periodicity on Stability

- Instabilities can be induced by
  - Decreasing sensitivity (increasing length scale of periodicity)
  - Reducing exothermicity
  - Diffusional inhibition
- Variation in types of instability
  - 1-D Oscillatory Combustion
  - 2-D Spinning Combustion
  - 3-D Chaotic

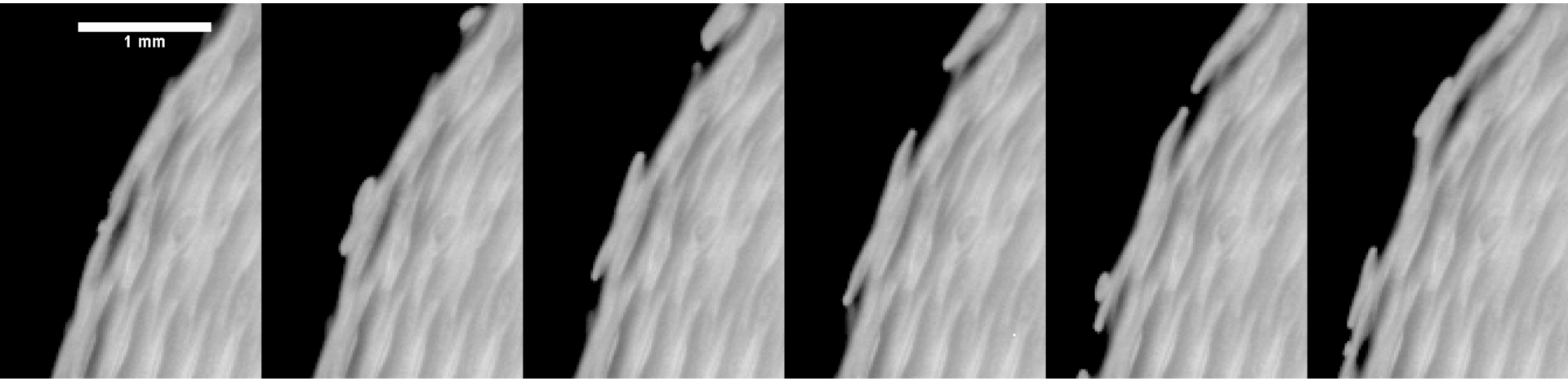

Still images from Co/Al with 250 nm bilayer thickness exhibiting 2-D “spinning” instability (80 μs between frames)

Experimental Plan

Vary *Le* and β to determine stability boundary

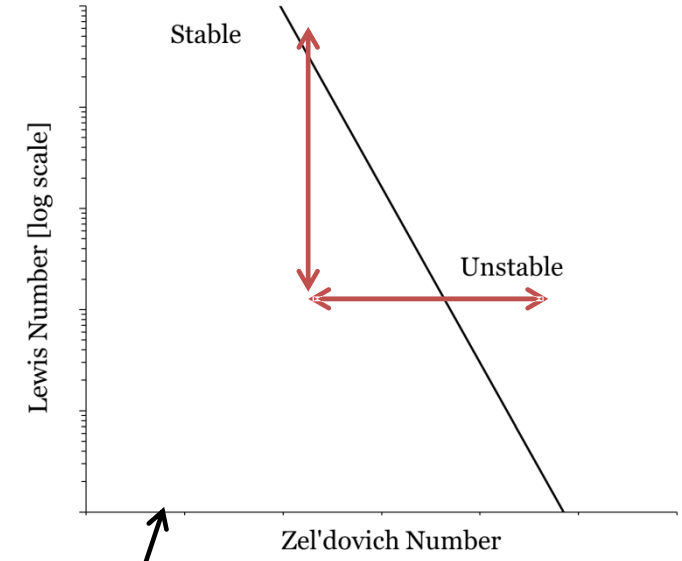

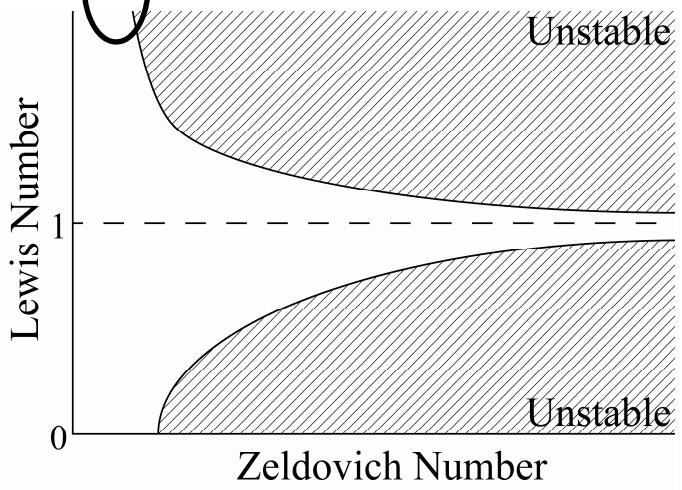

- Lewis Number, $\frac{\alpha}{D} = \frac{\kappa}{D\rho c}$
  - Vary *Le* by introducing diffusion barriers between reactants, decreasing D
- Zel'dovich Number,

  $\beta = \frac{E_a}{RT_{ad}{}^2}(T_{ad} - T_0)$
  - Reduce adiabatic flame temperature through dilution
  - Should NOT have a direct effect on *Le*

Experimental Material
Co/Al Nanolaminates

- $Co + Al \rightarrow CoAl; \Delta H_{calc} = -43 \frac{kJ}{mol_{atoms}}; \Delta H_{exp} = -54 \; to \; -61 \frac{kJ}{mol_{atoms}}$
  (de Boer et al, *Cohesion in Metals*, 1988)
- Co/Al nanolaminates stability vs. bilayer thickness behavior is known
  - 33.2 nm BL foils are stable, 66.4 nm BL foils are on cusp of stability

- Typical design of sputtered reactive foils
  - Macroscale stacks of nanometric metal layers
  - Clean interfaces, high purity materials

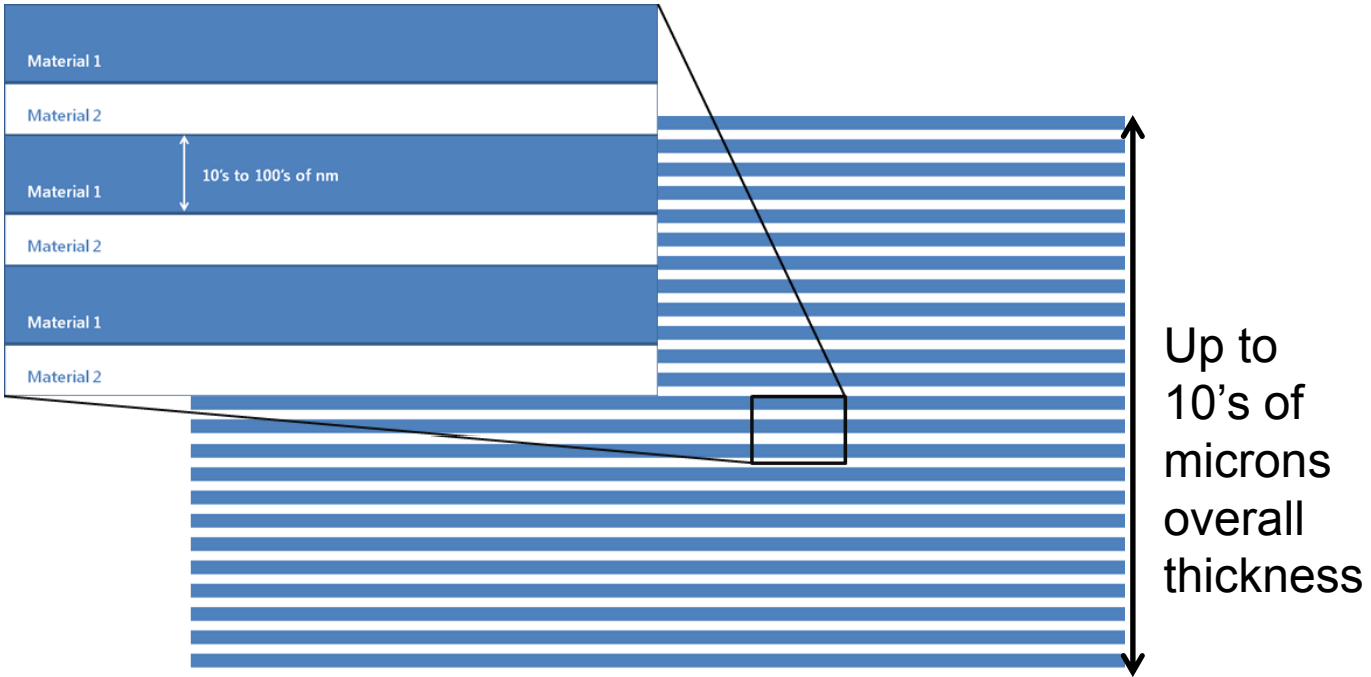

Multilayer Design

Diffusion Designs to vary *Le*

- Design for variation of *Le*
  - Sputter thin (1.0 to 3.0 nm) layer of reaction products at each reactive interface
  - CoAl alloy sputter targets allow precise control of barrier layer thickness
  - Total caloric potential of reactive multilayer maintained

- $Le = \frac{\alpha}{D}$ so increasing CoAl barriers decreases D, increasing *Le*

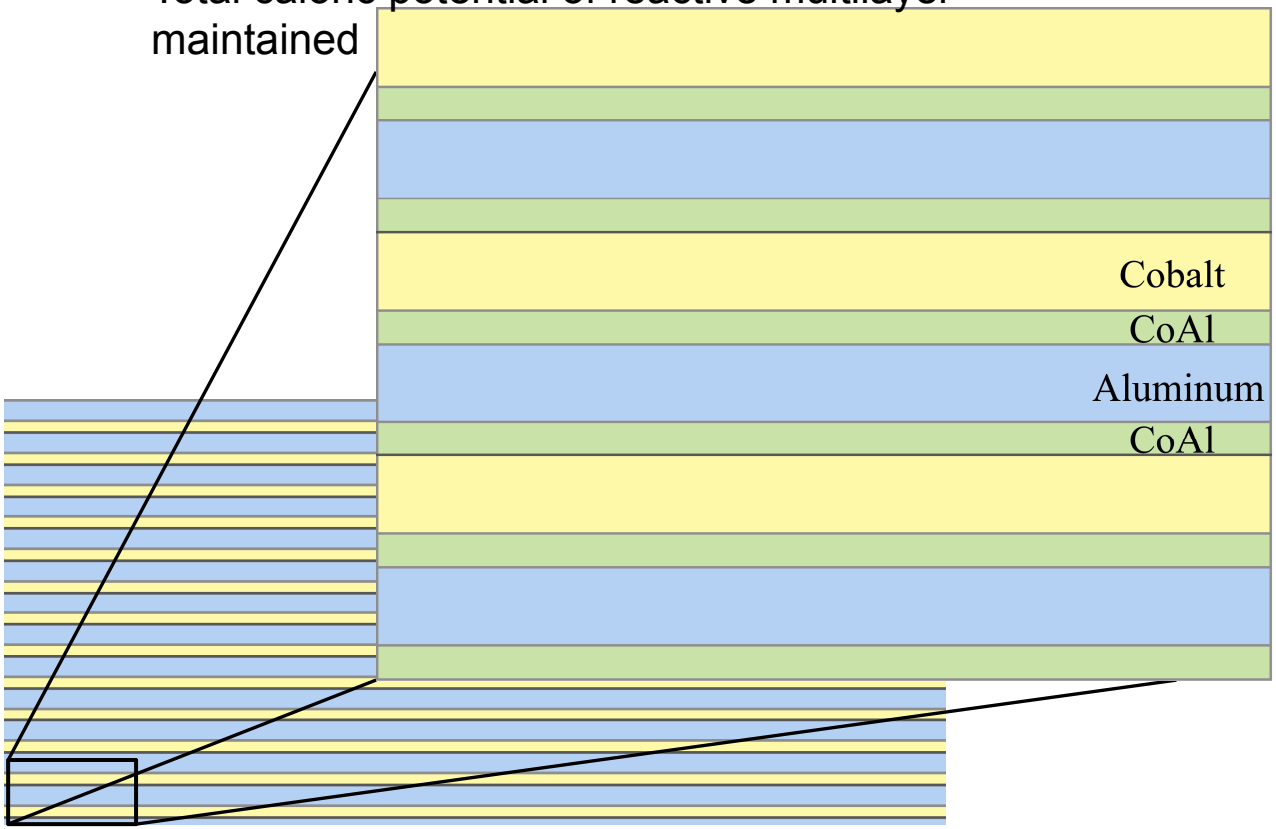

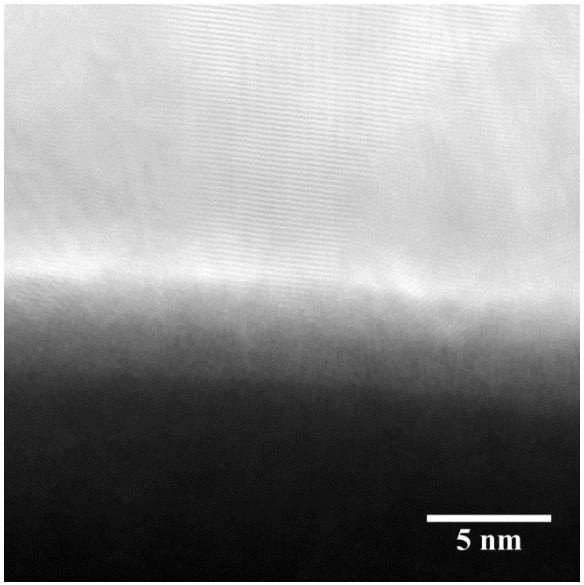

Multilayer Design
Dilution Designs to vary β

- Design for variation of β
  - Layers of CoAl product are deposited *within* each reactant layer
  - Reactive interfaces and diffusion distances are unchanged from the baseline multilayer design
  - Total volumetric dilution from 0% to 30%

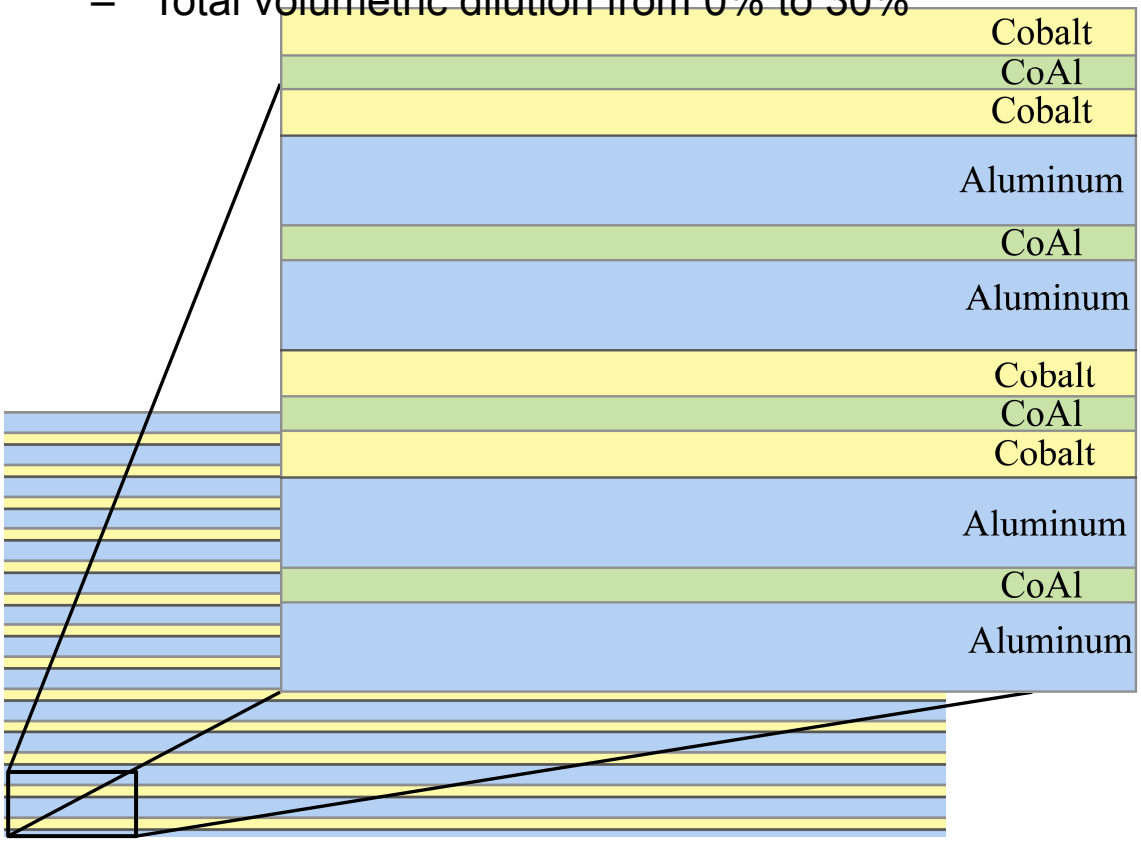

- $\beta = \frac{E_a}{RT_{ad}{}^2}(T_{ad} - T_0)$ so increasing CoAl dilution decreases T_{ad}, increasing β

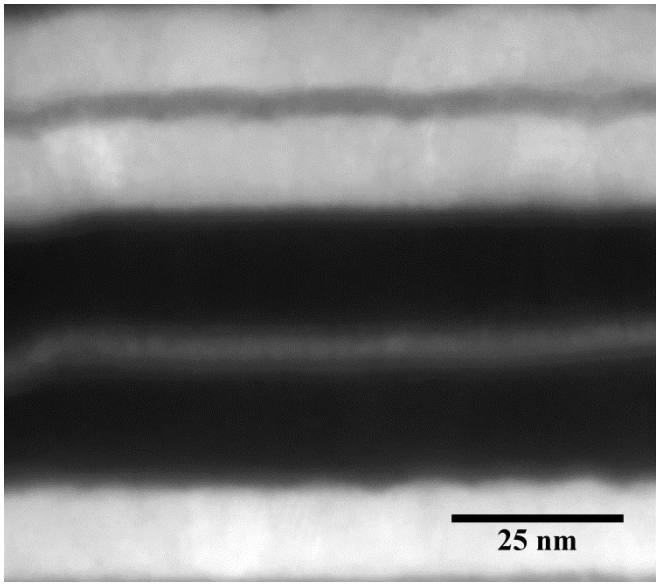

Calorimetry

Determination of ΔH and apparent E_a

33.2 nm BL				
Dilution [Volume Percentage]	Diffusion Layer Thickness [nm]	Activation Energy [kJ/mol atoms]	Heat Release [kJ/mol atoms]	Heat Release [% max]
0	0	28.2 ± 0.3	-39.1 ± 1.5	100
5.68	1	31.8 ± 1.1	-41.6 ± 2.1	106.5
11.36	2	35.5 ± 1.3	-40.4 ± 1	103.5
15.3	3	34.3 ± 2.2	-37.7 ± 1	96.3
10	0	31.2 ± 1	-33 ± 1.5	84.4
20	0	29.4 ± 0.9	-30.1 ± 0.9	77.1
30	0	33.2 ± 1.3	-27.9 ± 2.4	71.5
66.4 nm BL				
Dilution [Volume Percentage]	Diffusion Layer Thickness [nm]	Activation Energy [kJ/mol atoms]	Heat Release [kJ/mol atoms]	Heat Release [% max]
0	0	30.1 ± 0.5	-45.7 ± 1.4	100
2.93	1	33.1 ± 2.3	-43.5 ± 3.3	95.1
5.68	2	30.5 ± 2.2	-42.6 ± 1.7	93.2
9.39	3	33.8 ± 0.2	-41.2 ± 0.8	90.2
10	0	32.9 ± 3.3	-38 ± 2.3	83.1
20	0	33.8 ± 1.7	-30.9 ± 2.2	67.6
30	0	34.7 ± 0.8	-25.7 ± 1.3	56.2

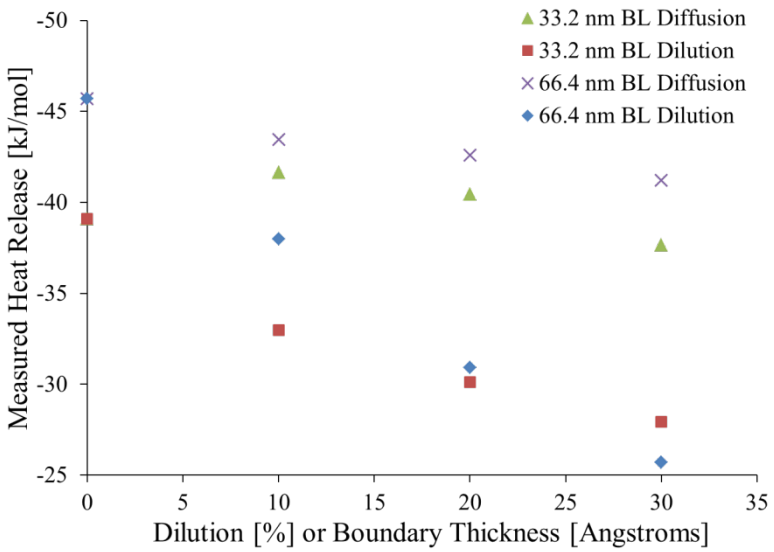

- Heat release directly measured from DSC
- Apparent E_a determined by Kissinger method

Calculation of T_b and resulting Zel'dovich number

- T_{ad} calculated from measured ΔH, using constant c of CoAl, 570.5 J/(kg·K)

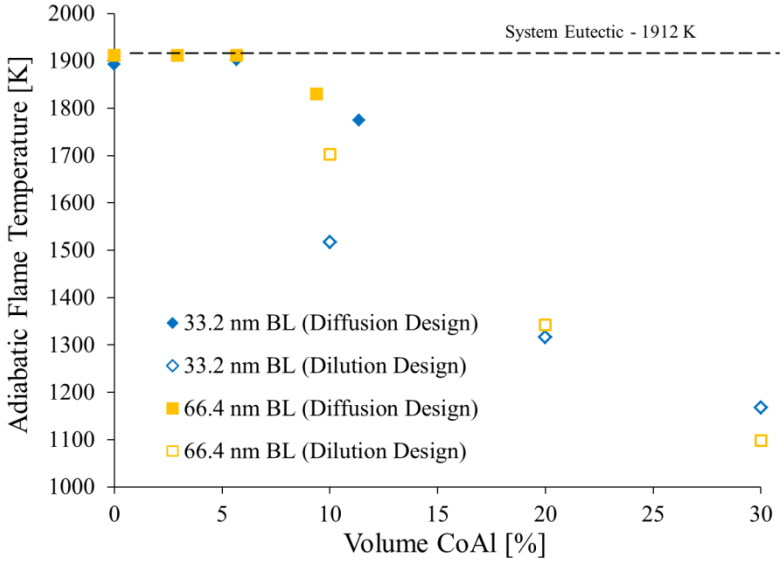

- β ranges from:

  33.2 nm BL
  - 1.8 to 2.5 for diffusion designs
  - 1.8 to 3.4 for dilution designs

  66.4 nm BL
  - 1.9 to 2.2 for diffusion designs
  - 1.9 to 3.7 for dilution designs

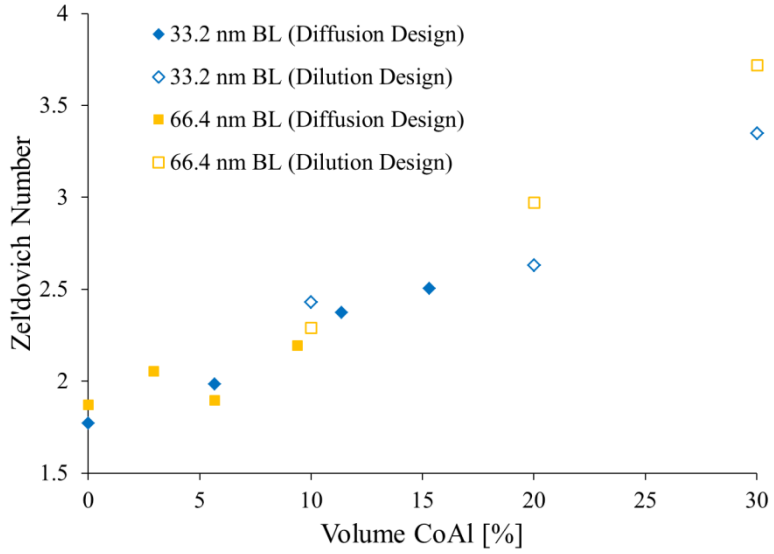

Propagation Rates
Diffusion Barriers

Co/Al Nanolaminates
33.2 nm Bilayer Thickness
CoAl Alloy Barrier Deposited
at Co+Al Reactive Interface
Barrier Thickness Noted
Air Pressure = 10.0 mTorr

1 s Real Time = 1 ms Reaction Time

Co/Al Nanolaminates
66.4 nm Bilayer Thickness
CoAl Alloy Barrier Deposited
at Co+Al Reactive Interface
Barrier Thickness Noted
Air Pressure = 10.0 mTorr

1 s Real Time = 1 ms Reaction Time

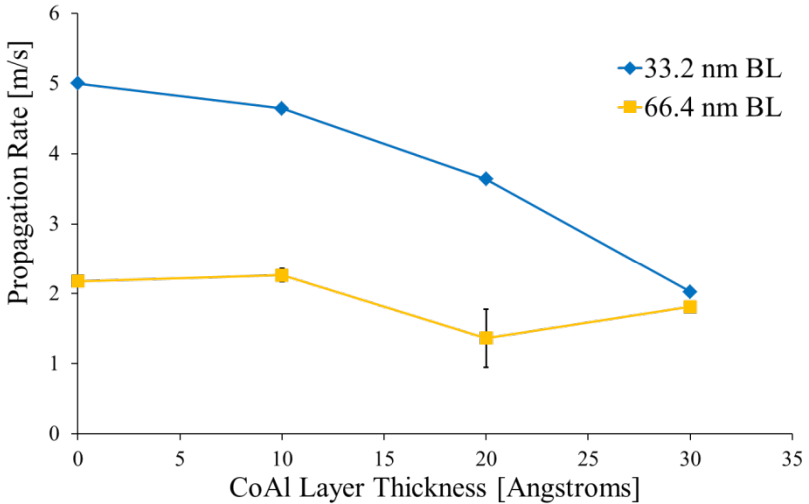

Diffusion – Reaction Front Stability

33.2 nm BL

1.0 nm Barrier–
Stable front, *u* = 4.64 m/s
2.0 nm Barrier–
Stable reaction front,
u = 3.64 m/s
3.0 nm Barrier–
Spin instability appears, *u* = 2.03 m/s

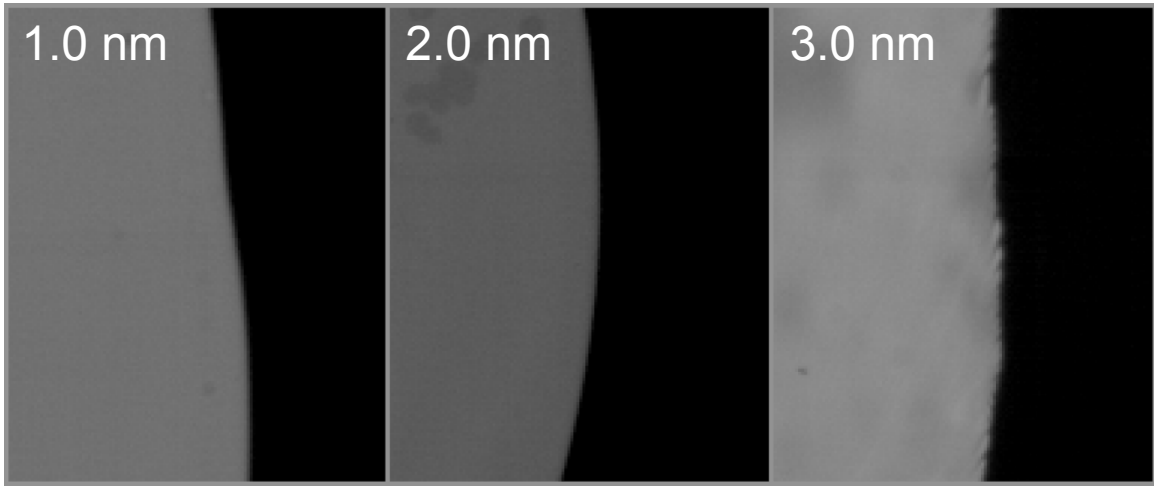

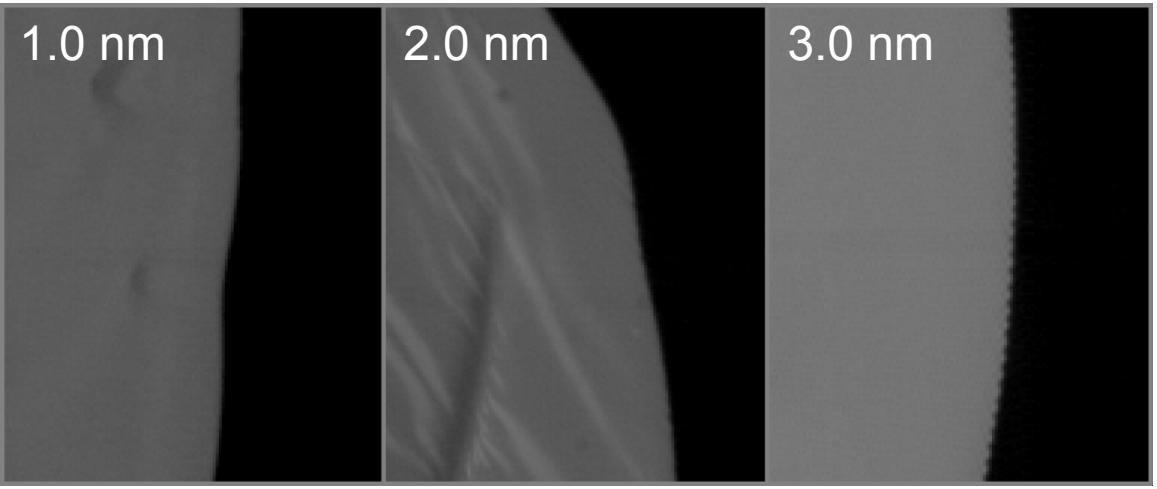

66.4 nm BL

1.0 nm Barrier –
Stable reaction front, *u* = 2.27

2.0 nm Barrier–
Slight instability in front,
u = 1.36 m/s

3.0 nm Barrier–
Spin instability appears, *u* = 1.81 m/s

Propagation Rates
Dilution Designs

Co/Al Nanolaminates
33.2 nm BL Th.
Diluted with CoAl Alloy
Volumetric Percent CoAl Noted
Air Pressure = 10.0 mTorr

1 s Real Time = 1 ms Reaction Time

Co/Al Nanolaminates
66.4 nm BL Th.
Diluted with CoAl Alloy
Volumetric Percent CoAl Noted
Air Pressure = 10.0 mTorr

1 s Real Time = 1 ms Reaction Time

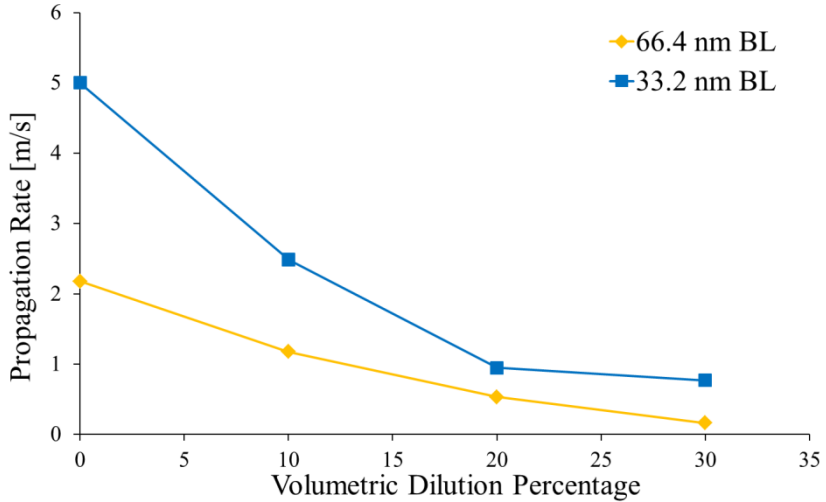

Dilution– Reaction Front Stability

33.2 nm BL

10% Dilution –
Stable front, u = 2.49 m/s

20% Dilution –
Spin instability appears, u = 0.95 m/s

30% Dilution –
Spin instability is more apparent, u = 0.77 m/s

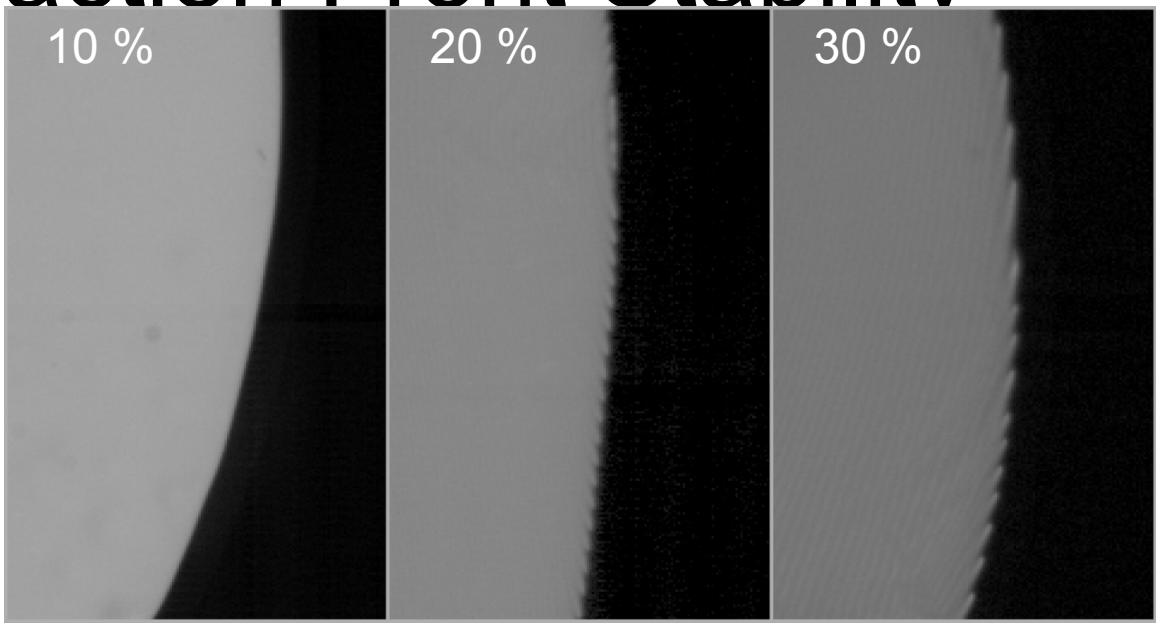

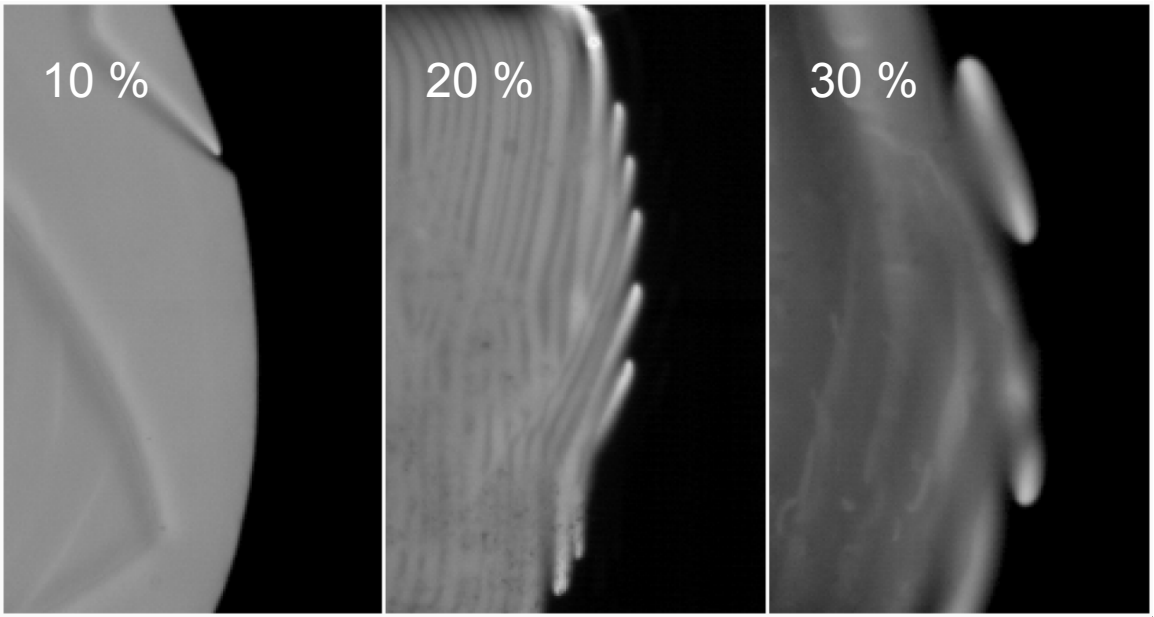

66.4 nm BL

10% Dilution –
Spin instability appears, u = 1.18 m/s

20% Dilution –
Spin instability appears, u = 0.53 m/s

30% Dilution –
Spin instability becomes very large and irregular, u = 0.16 m/s

Experimental stability vs. analytical stability criteria

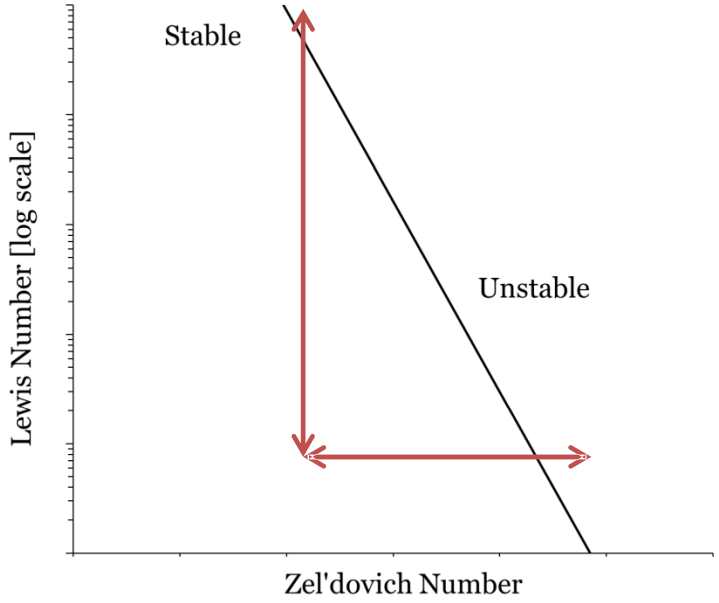

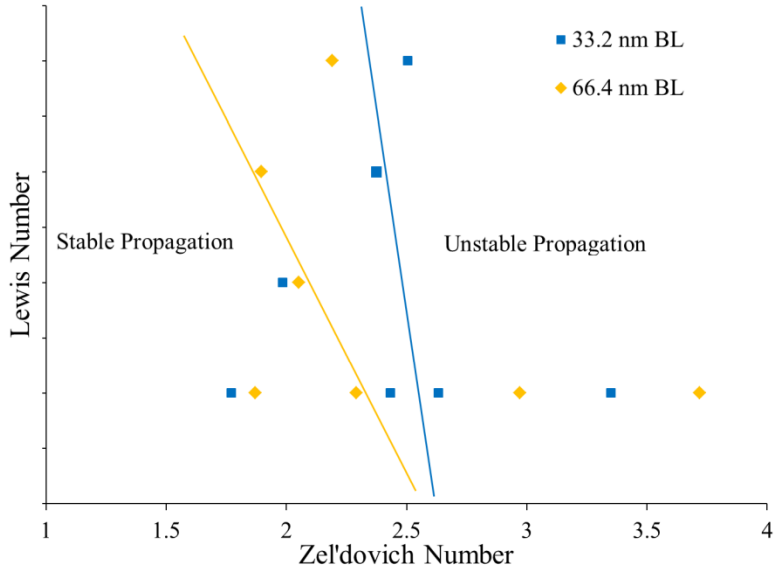

- Plotting on *Le*-β axes, ranking data by *Le* get approximate regions of stability
- Not identical between BL designs

Conclusions

- Can grow thin films that can well isolate effects of diffusion and mass dilution
- Variation in *Le* and β can introduce reaction instabilities, as predicted by theory
- Induced instabilities in Co/Al laminates limited to 2-D spinning instability
- Similar but not identical stability limits between BL designs

Reactivity Enhancement and Control

- Ball-milling has been shown to reduce reaction initiation temperature in DTA testing of Ni-Al powder mixtures and can initiate self-sustaining reactions (Cardellini et al, 1994, 1996)
- Many materials have been processed, including B-Ti, B-Zr, Al-CuO, Al-Hf, Al-MoO_3, etc (Driezin et al, 2007)
- In this study, a Retsch PM100 planetary ball mill was used for high-energy ball milling (HEBM)
- Use of nano-particles has also been studied considerably for enhancing reactive system performance
  - Used in thermite systems (Son, 2007)
  - Intermetallic forming systems (Hunt, 2004)
  - Rocket propellants
  - Explosives

F. Cardellini, G. Mazzone, A. Montone, M. V. Antisari, *Acta Metall. Mater.* 42, 2445 (Jul, 1994)
F. Cardellini, G. Mazzone, M. V. Antisari, *Acta Materialia* 44, 1511 (Apr, 1996)
E.L. Driezen, et al, *Theory and Practice of Energetic Materials Vol .VII, 2007 Int'l Autumn Seminar,* 314 (2007)
S. F. Son, R. A. Yetter, and V. Yang, Journal of Propulsion and Power 23, 643 (2007)
E. M. Hunt, J. J. Granier, K. B. Plantier, et al., Journal of Materials Research 19, 3028 (2004).

Methodology

- In this study, we compare the following morphologies:
  - Unmodified Ni clad Al (Al size 50 micron, Ni/Al 70/30%wt)
  - High Energy Ball Milling (HEBM) of Ni/Al powders
  - Reduction of material size from micron to nano-particles
    - 80 nm Al (Novacentrix)
    - 80 -150 nm Ni (VWR)
- Thermal initiation was studied using Differential Thermal Analysis (DTA)
- Mechanical initiation was studied using Asay shear impact tests

SEM Micrographs – Ball Milled Material

Agglomeration caused by prevalence of cold welding in material due to absence of PCA

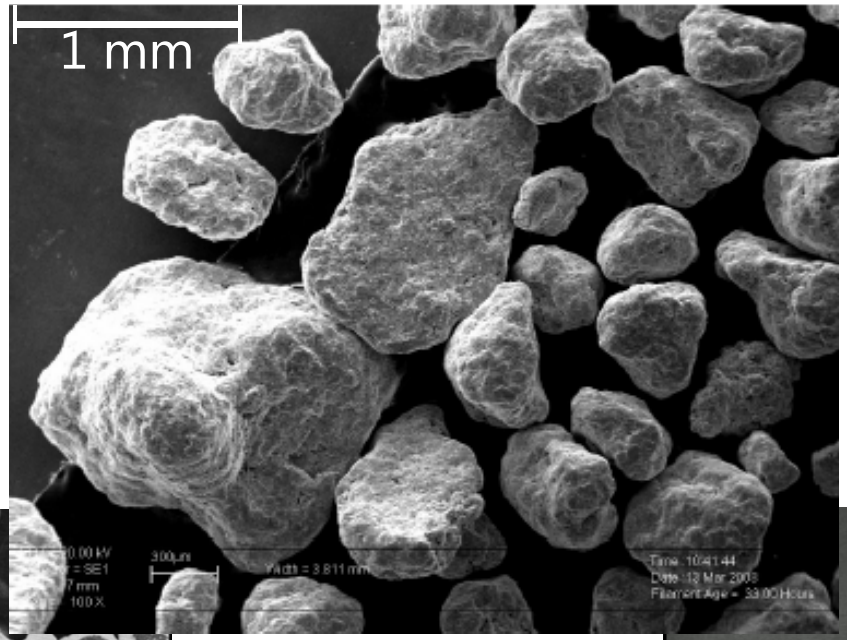

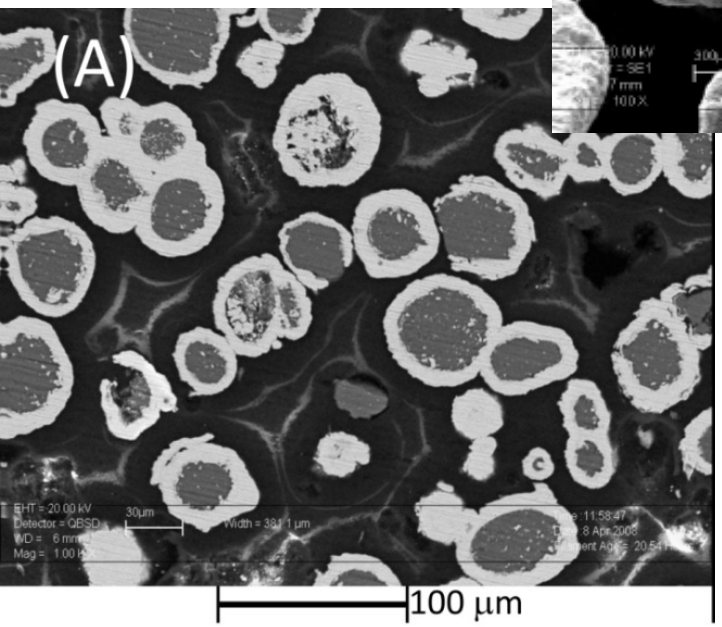

Cross Section

A) Section of baseline clad material

B) Cross section of aggregates, post-miling

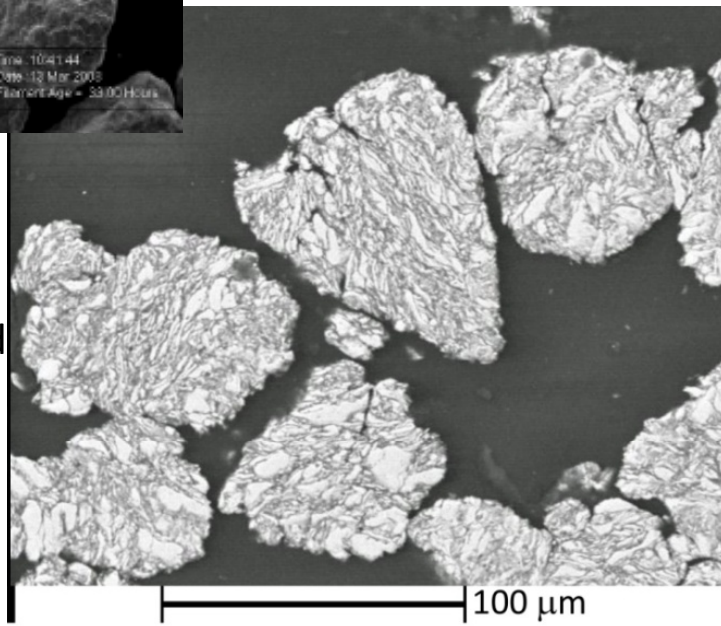

TEM microstructural investigation
Structural Refinement

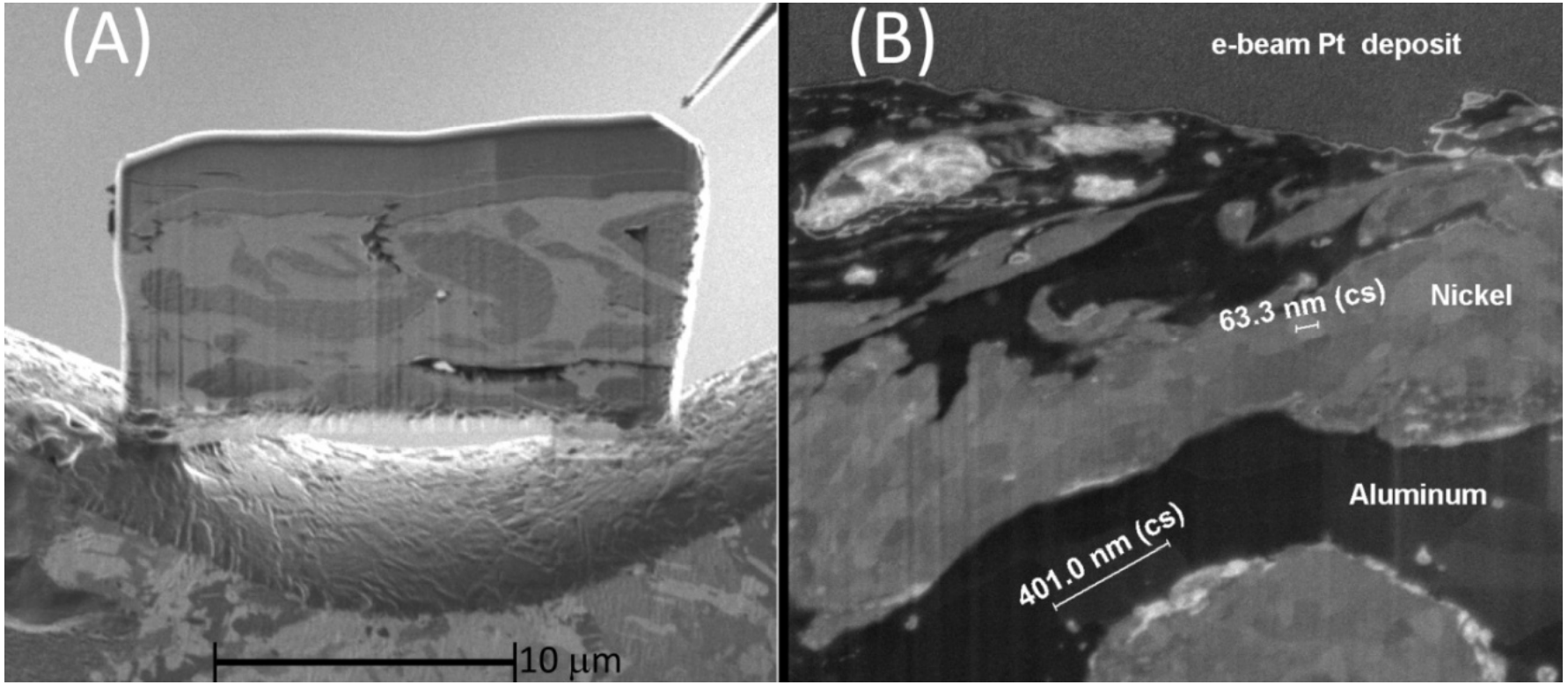

- Ion milled section removed from HEBM particle using Focused Ion Beam
- Removed section placed on TEM grid and imaged using FEI Titan STEM
- Extreme refinement of Al seen, but Ni thickness not reduced tremendously
- Many locations where Al flow entrains and thins Ni cladding

TEM microstructural investigation
Al/Ni Interface Characteristics

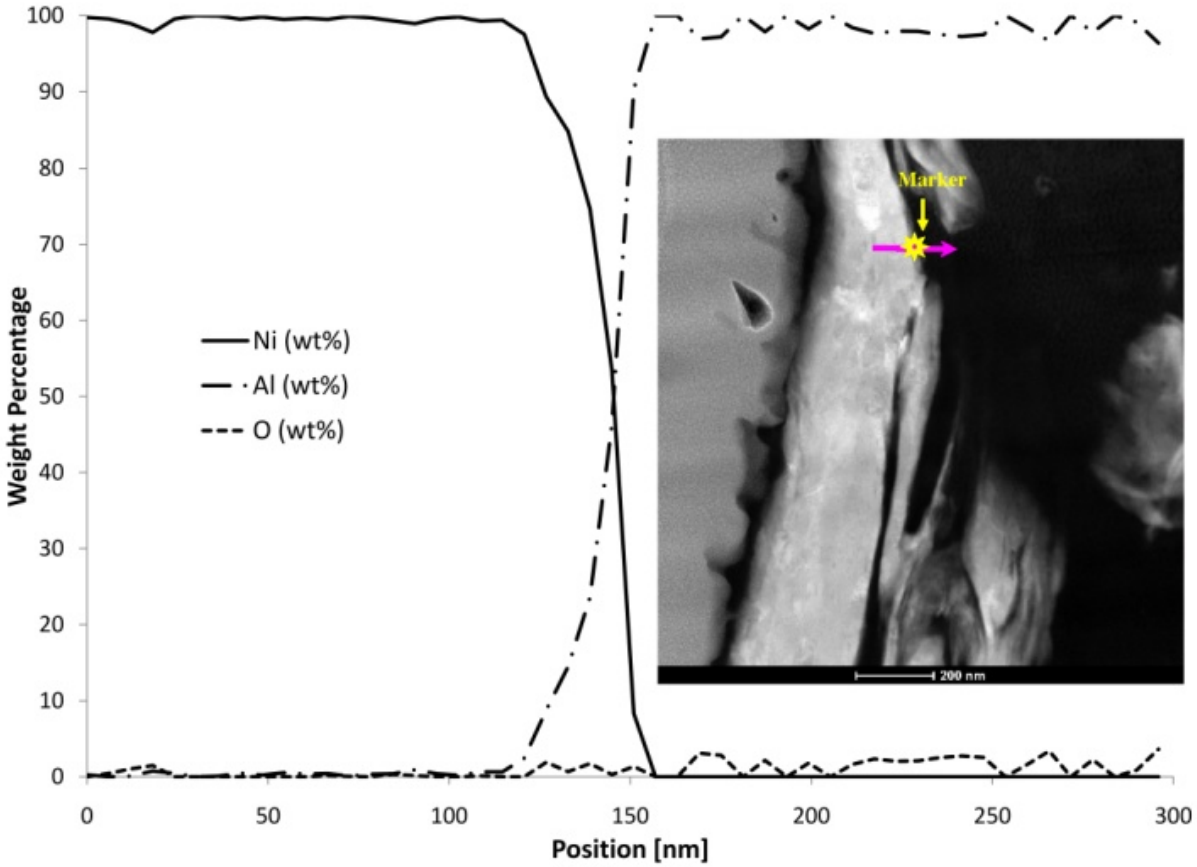

- EDS performed across Al/Ni interface
- No significant O content seen in this location
- Indicates that Al/Ni reactive interface does not have an oxide layer to act as an energy barrier to reaction

TEM microstructural investigation
Crystal structure – At interface

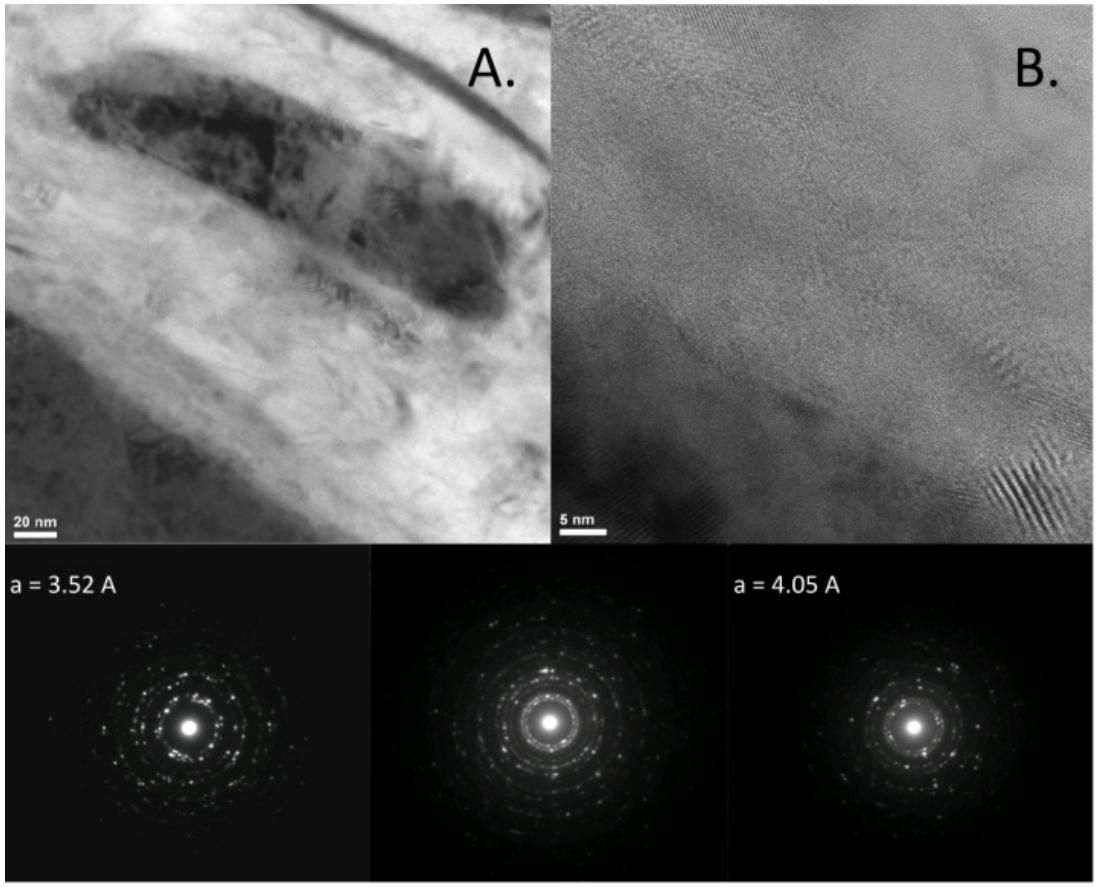

- ~20 nm crystallites of Ni seen embedded in Al near interface surface
- Create regions of high specific surface area at interface
- Again, no oxide barrier present

TEM microstructural investigation
Crystal structure – At interface

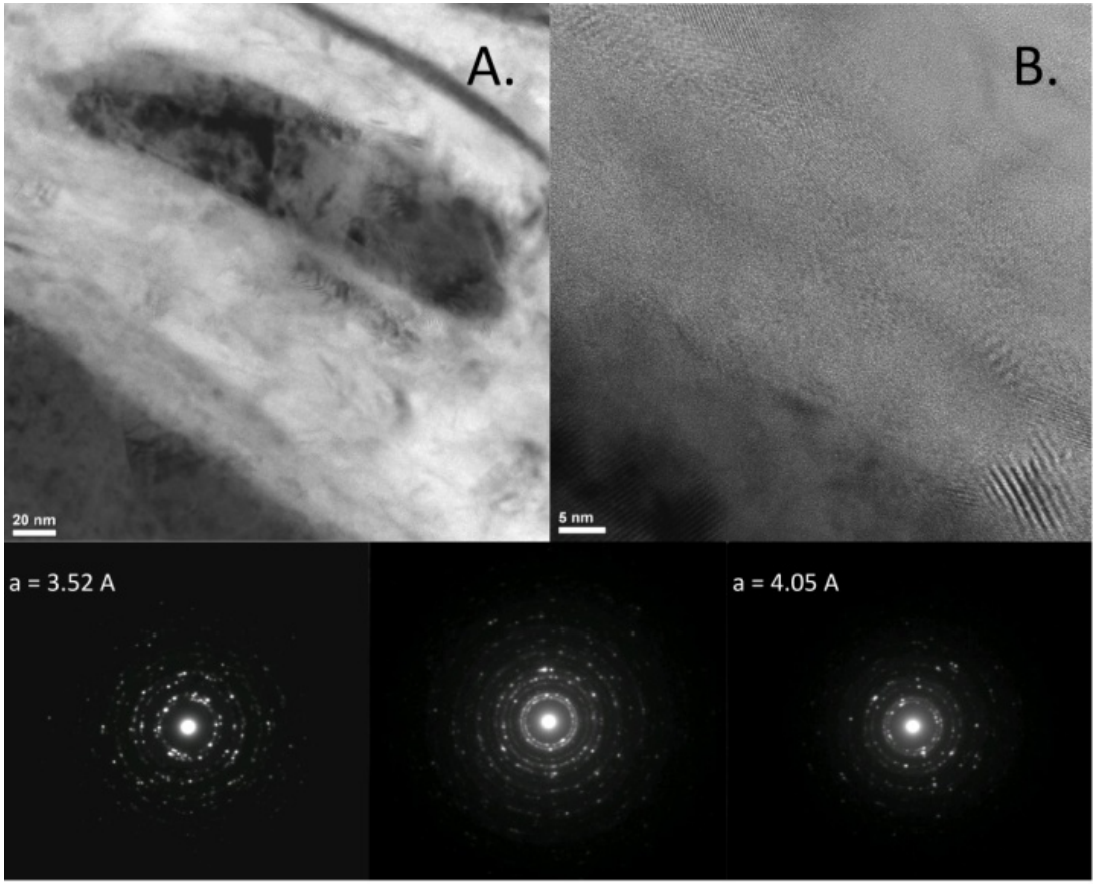

- Lattice distortion near surface (B) indicates strain, but no significant defect formation
- Diffraction rings shows only Ni fcc structure (left), Al fcc structure (right)
- Center diffraction pattern indicates only combination of Al and Ni fcc structures

DTA Analysis –

Milling materials and nanomaterials

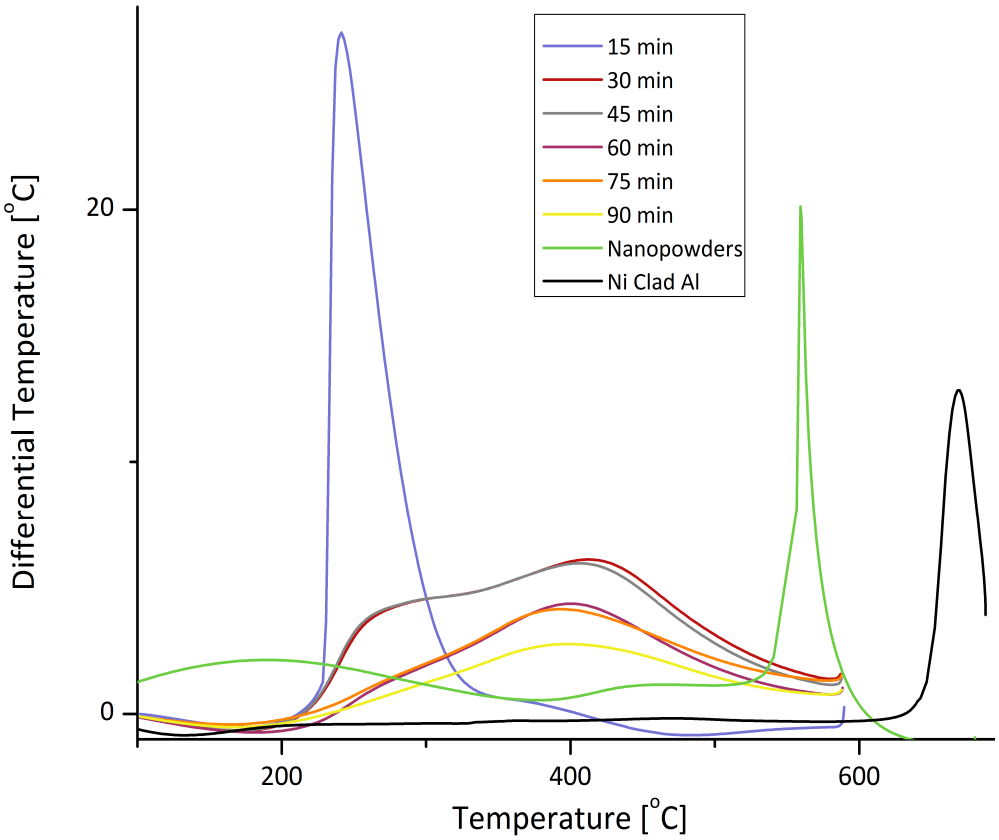

- Ignition temperature for TE reduced to ~220°C (593 K)
- Plot shows DTA traces (50 K/s) for various wet grinding times
- Arrived at optimal MA and wet grind time
- At 15 min MA and 15 min WG, TE mode is exhibited at DTA heating rates (50 K/s)
- Nanopowder mixture exhibits TE at 559°C (832 K)
- Can produce TE in milled materials at much lower temps

Gas Gun Testing

- 1” Gas Gun at Purdue
- Max muzzle energy ~ 50 kJ
- Velocities up to 1.1 km/s
- Target section designed for Asay shear test

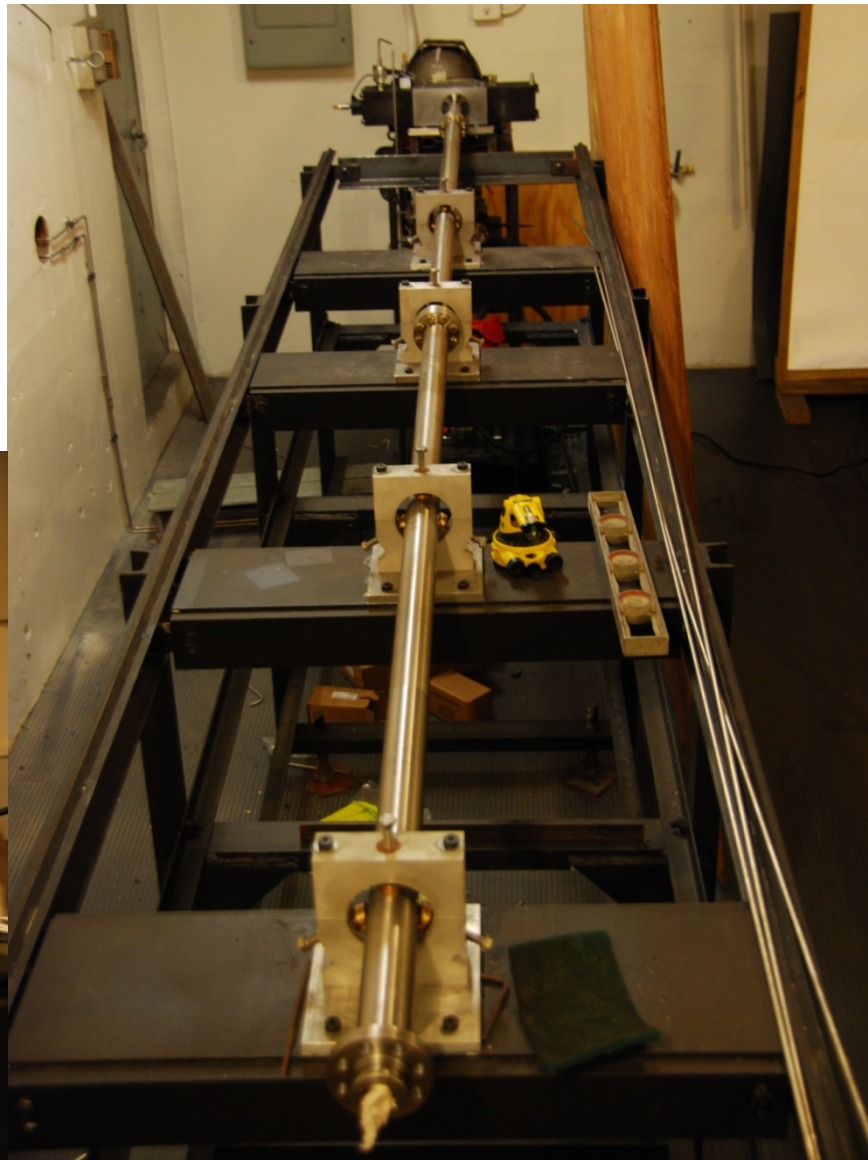

Gas Gun Testing

- Asay shear impact test utilized
  - Sample holder designed to create compressive and shear stresses in sample.
  - Plunger geometry can be varied to change strain field
  - Sample holders limit max impact velocity
  - 2D strain not maintained at high velocity
- Samples tested at 65-67%TMD
  - Nanopowder mixtures
  - HEBM mixture

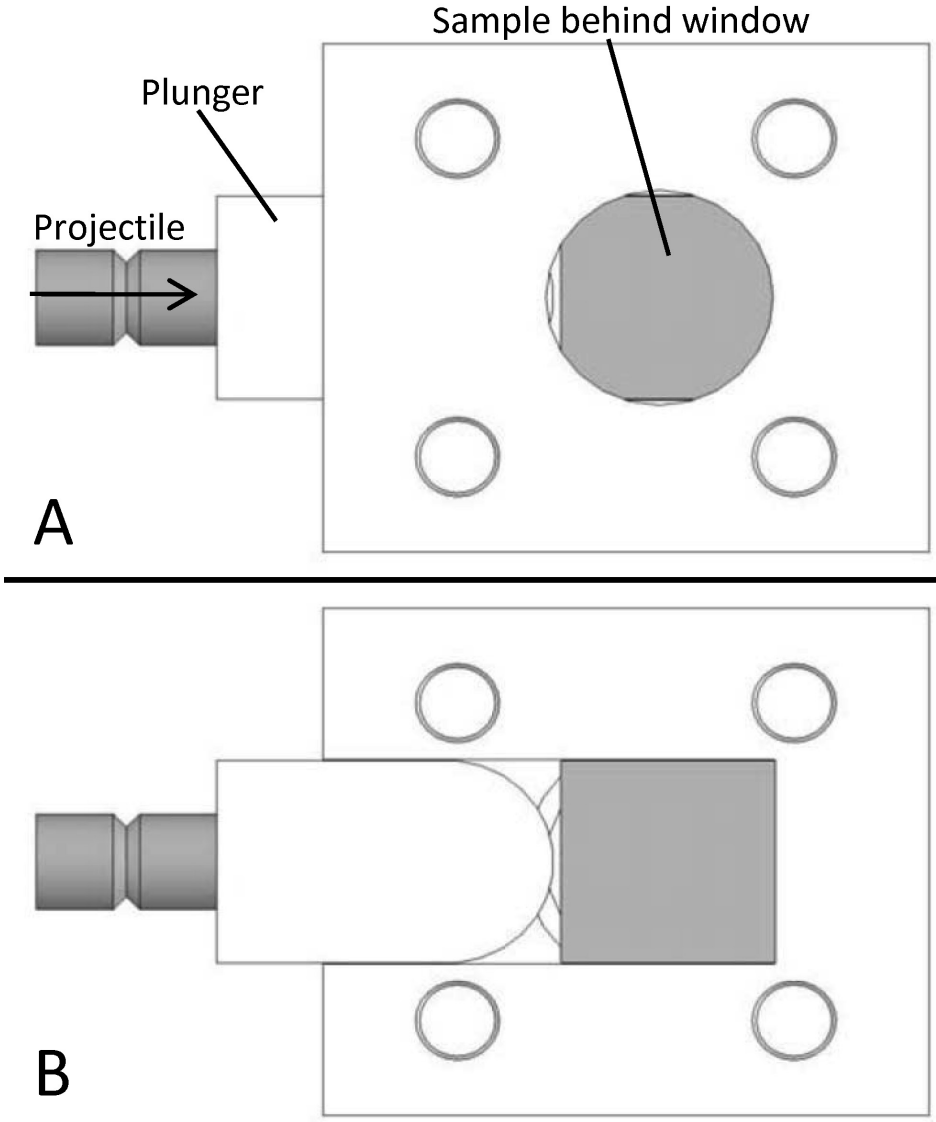

B. W. Asay *et al.*, in Shock Compresssion of Condensed Matter, (1997), pp. 567

Gas Gun Testing

- Two distinct reaction modes in nano-powder mixtures
- Slow mode –Delay time ~30 ms, followed by autowave with propagation rate of ~6 cm/s

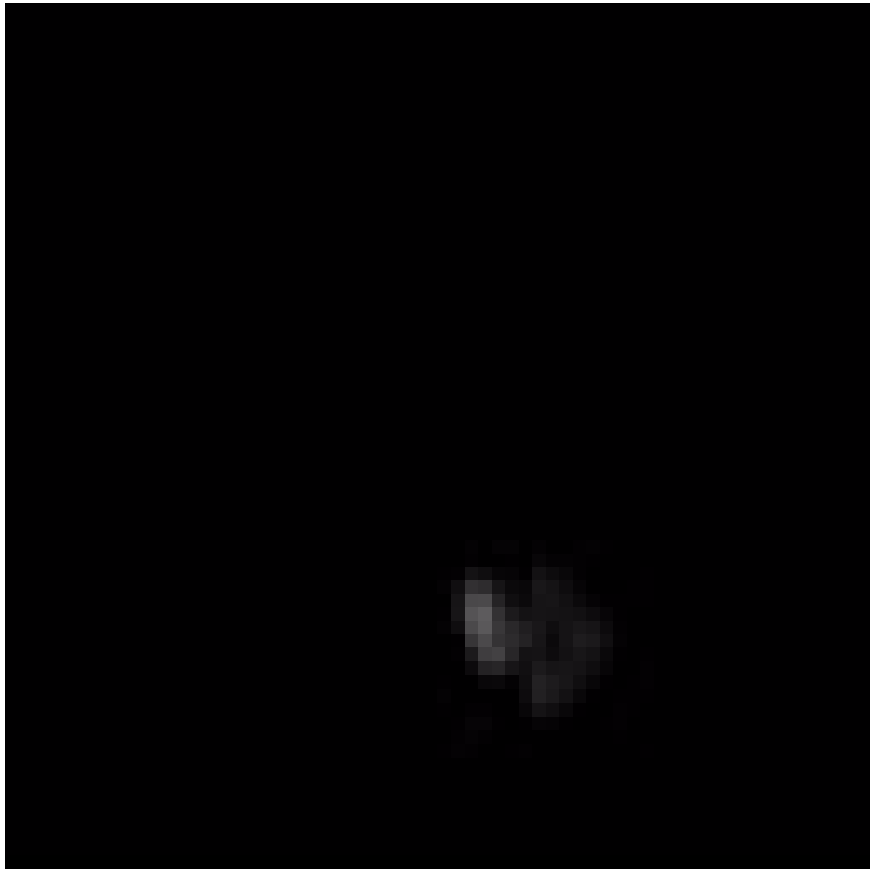

Gas Gun Testing - Nano Powders

- Fast reaction mode -
  - Appeared at 840 m/s impact (8.6 kJ), mixed with slow mode
  - Fast mode consumes nearly entire sample at 1070 m/s impact (14.9 kJ)
- Initially appears to move at speed of impact
- Fast mode slows, like overdriven shock

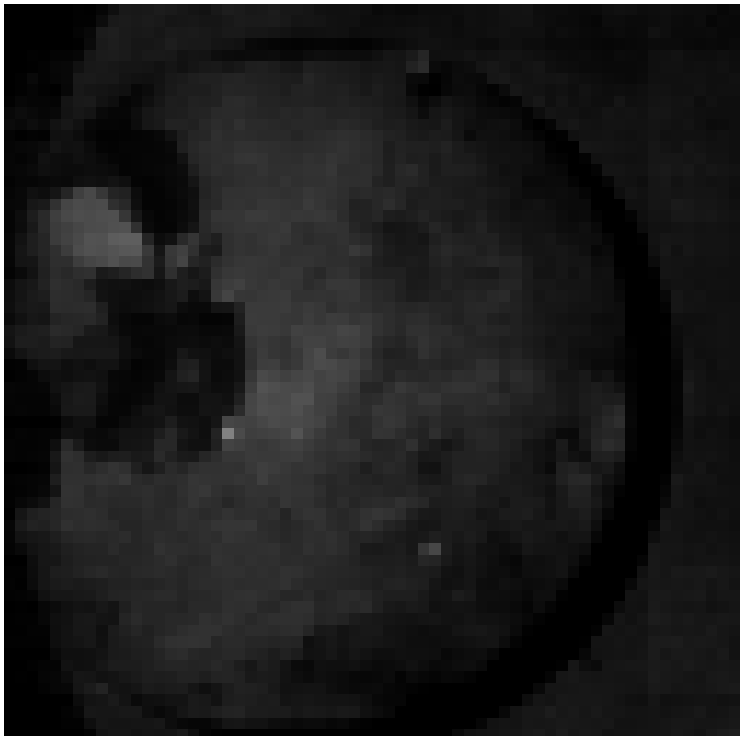

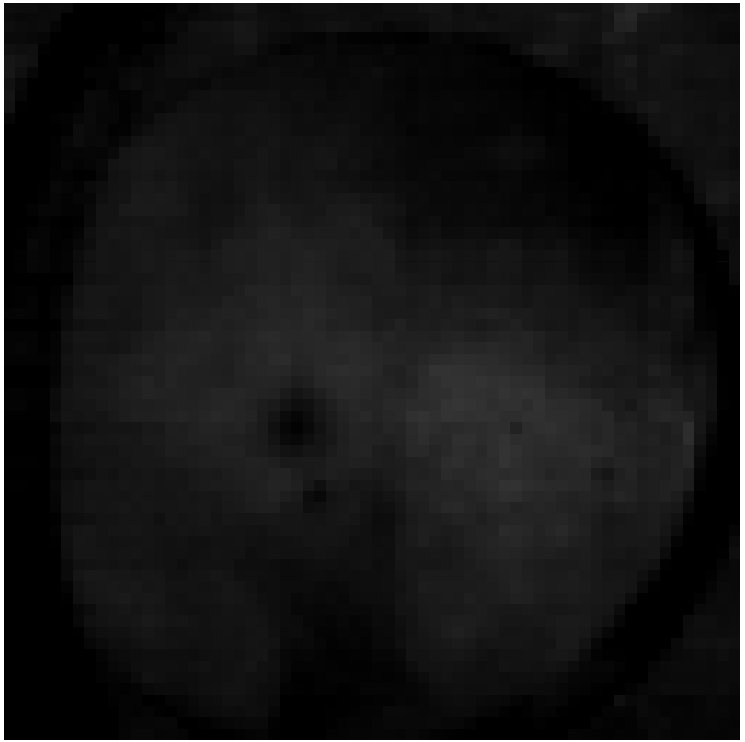

Gas Gun Testing - Nano Powders

- Fast reaction mode -
  - Appeared at 840 m/s impact (8.6 kJ), mixed with slow mode
  - Fast mode consumes nearly entire sample at 1070 m/s impact (14.9 kJ)
- Initially appears to move at speed of impact then slows, like overdriven shock
- Interpreted as mechanically induced thermal explosion

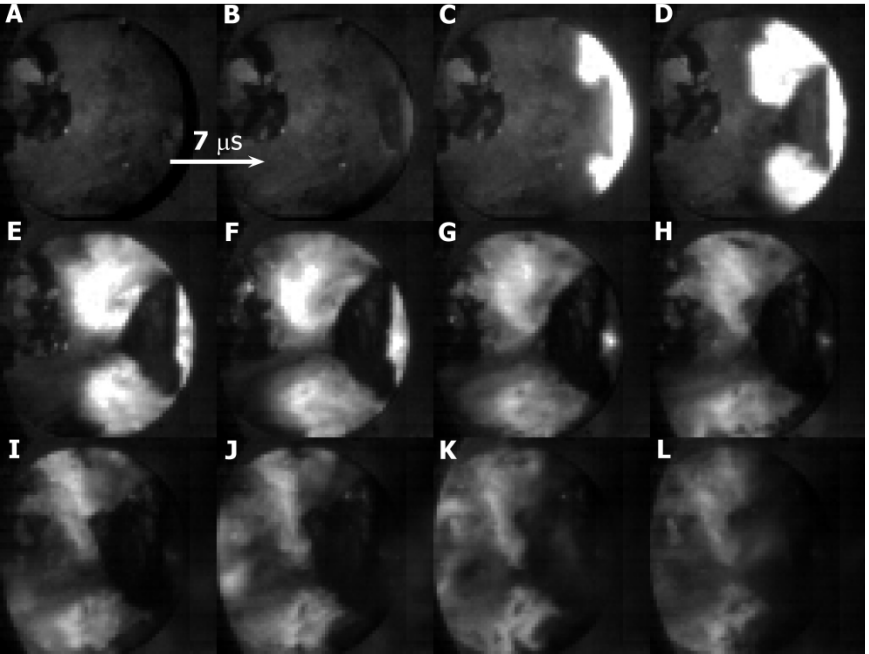

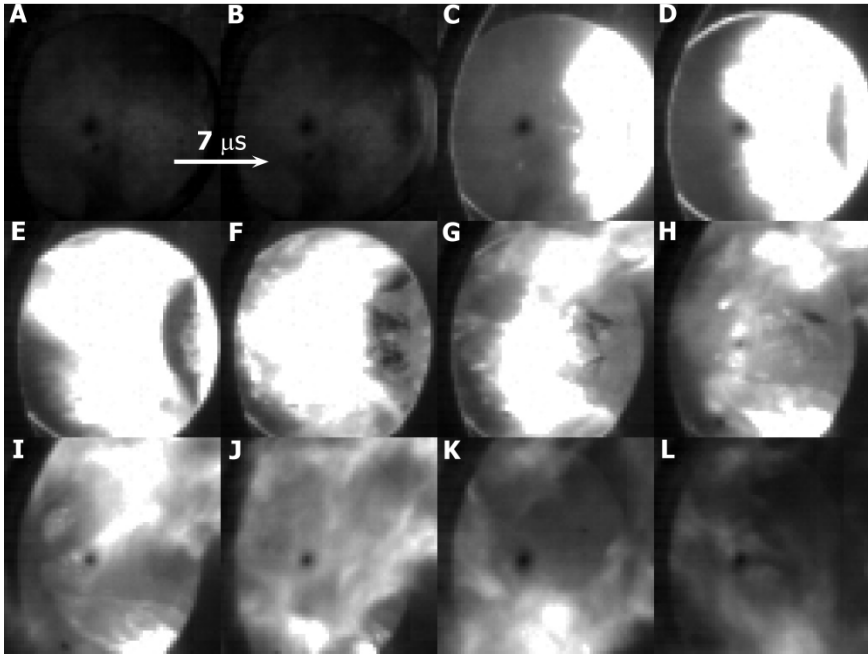

Shear Bands in Reaction Mode Selection

- In mixed mode case, fast reaction mode is seen above and below the rounded plunger, not along the axis
- Shear strains are more prevalent than compressive strains in these zones, due to geometry of plunger
- Combination of mixing (high shear) and rapid heating (pore collapse and plastic shear) allows selection of fast reaction mode

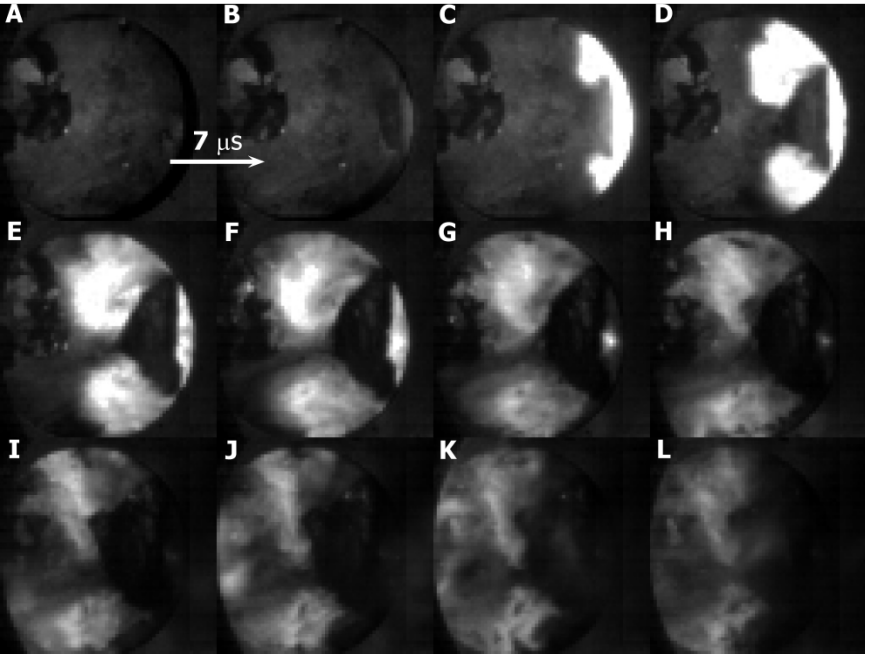

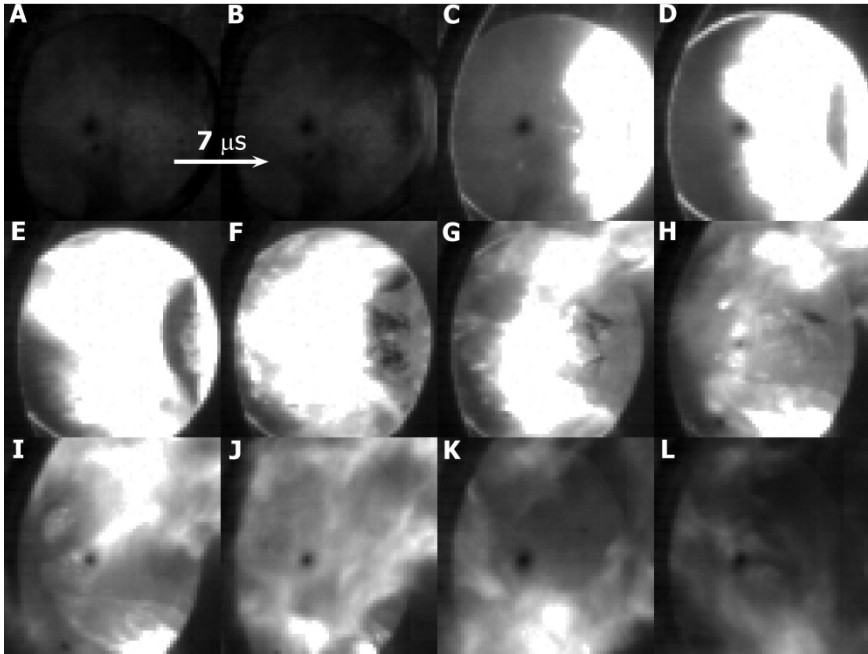

Gas Gun Testing

HEBM Material –Impact Vel. 715 m/s (6.08 kJ)

- Ni/Al milled for 15 min. at charge ratio of 5:1, then wet ground to reduce particle size to d< 25 μm
- %TMD from 65 to 70%, similar to nanopowder samples
- No reaction during impact, no shear banding apparent.
- SHS reaction initiation occurs after 17 ms induction period

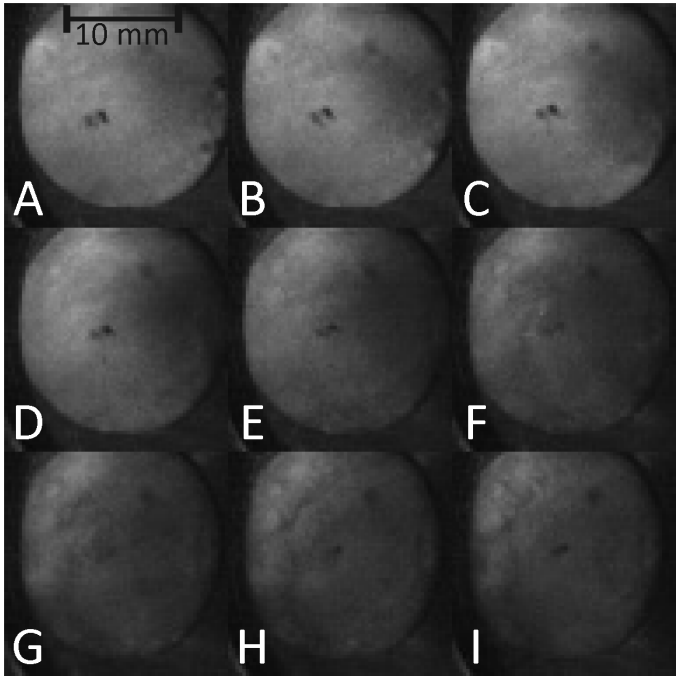

Impact of sample (7 μs between frames)

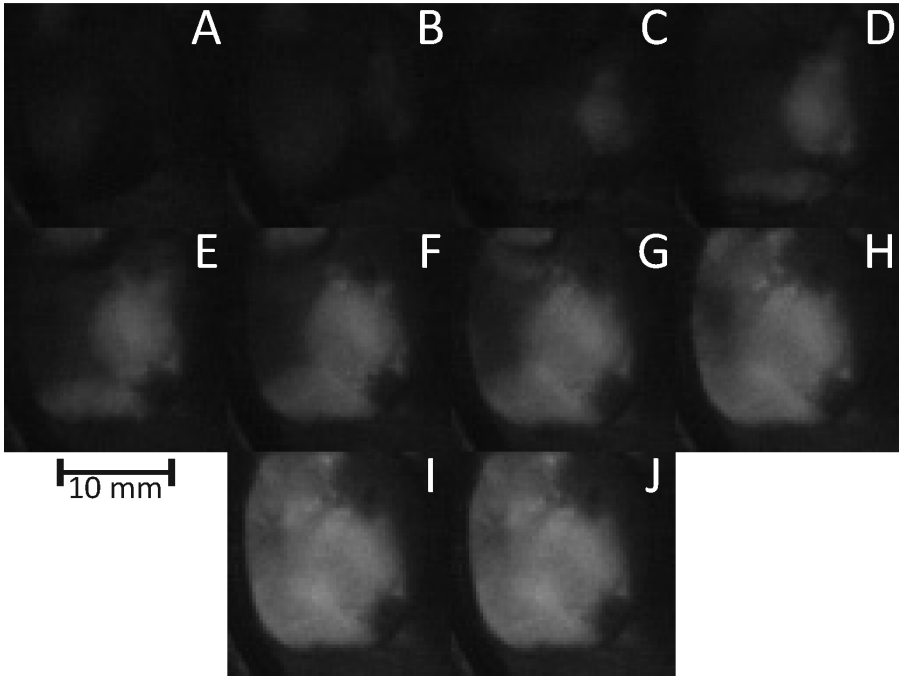

Reaction of sample (7 ms between frames)

Gas Gun Testing

HEBM Material –Impact Vel. 794 m/s (7.50 kJ)

- Shear Bands appear during impact
- Local, non-propagating reactions appear in shear bands with short residence times (~14 μs)
- Slow reaction mode occurs after induction period, as before

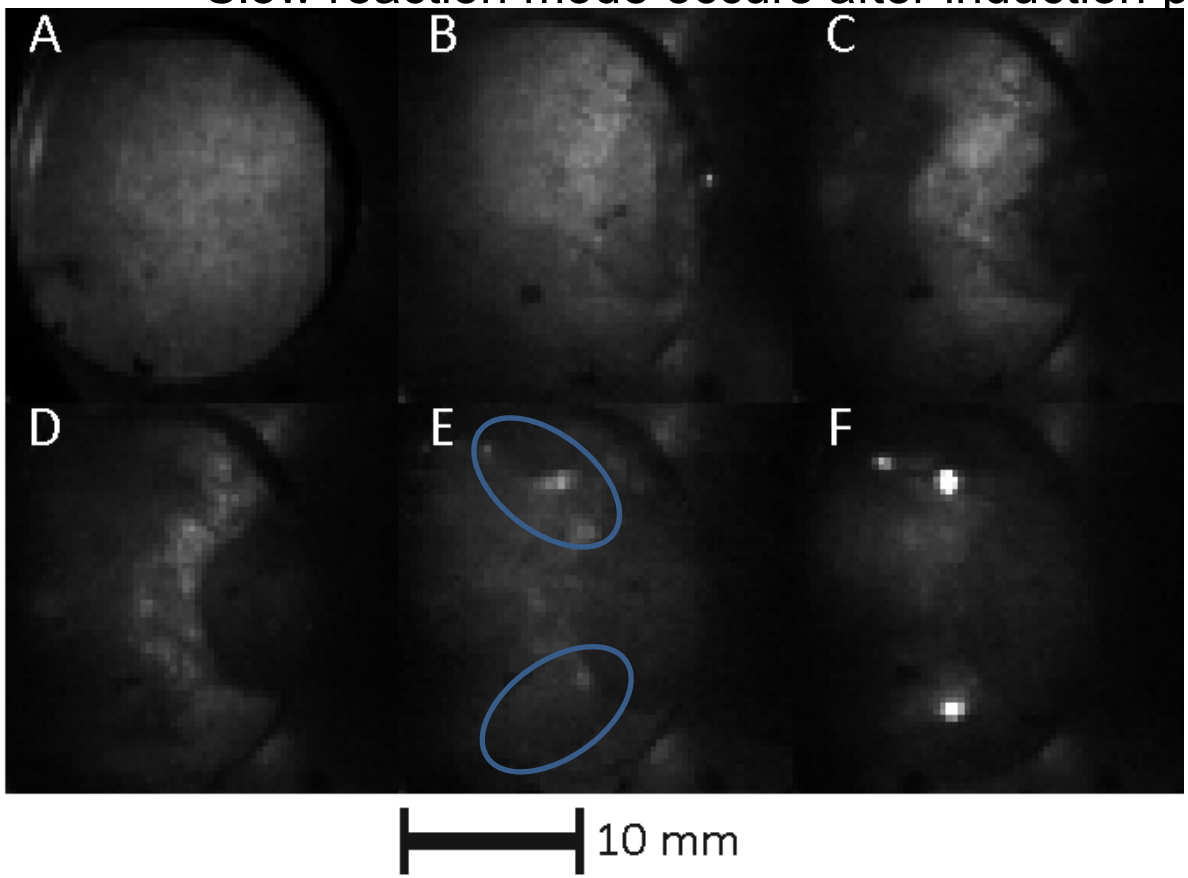

- Shear bands form during impact, circled in frame E
- Local ignition initiate in shear bands in frame E. in frame F, reaction zones are clearly apparent.

(7 μs between frames)

Heat diffusion distance

- For nano-scale powder mixtures, porosity is intimate with interfacial areas
- For HEBM materials, porosity is distant from most interfacial areas
  - Time is necessary to transfer heat from pore collapse to reactive areas

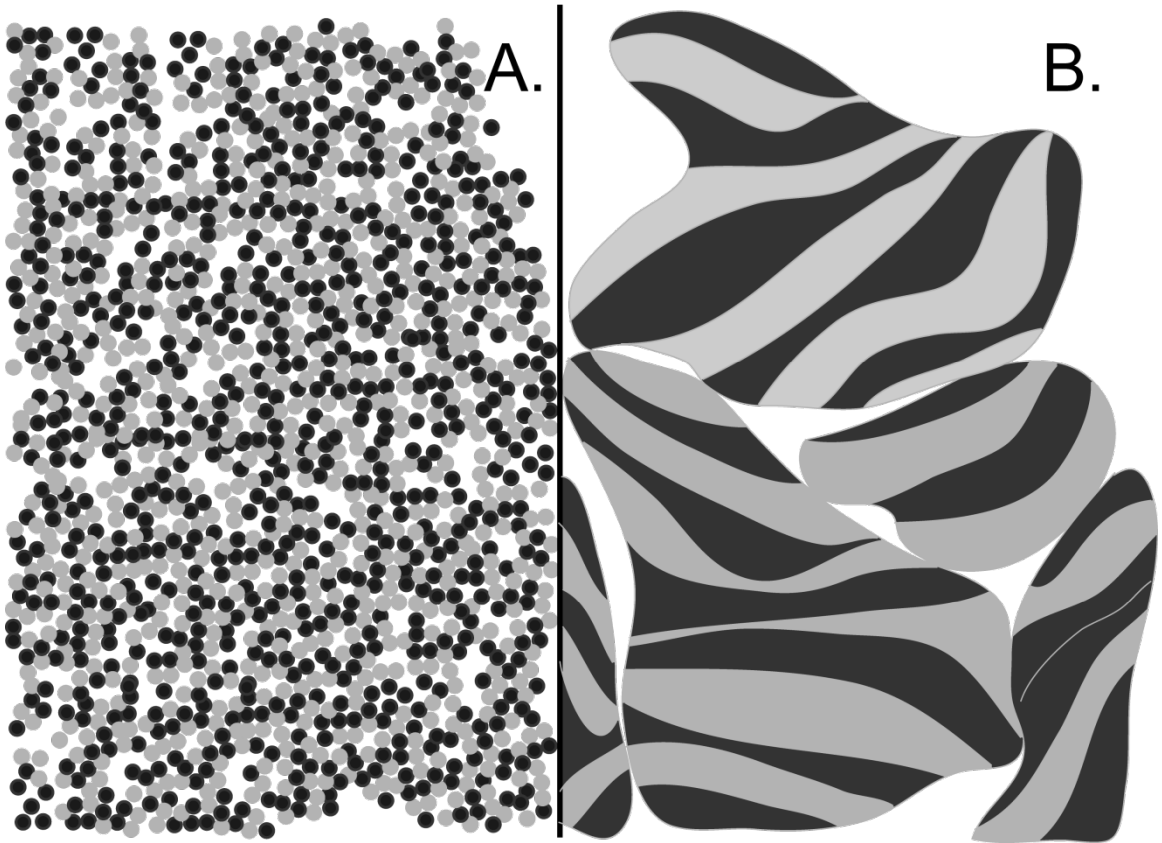

Summary of Ni/Al Results

- Reactivity enhancement methods can *CONTROLLABLY* lower ignition temperature in Ni/Al system in both nano and HEBM mixtures
- HEBM produces different reactivity effects than particle size reduction
  - HEBM can reduce temperature for thermal initiation more effectively than reducing particle size
  - Nanopowder mixtures more sensitive to mechanical impact – likely due to colocation of porosity and reactive interface
- Thermal explosion mode seen in mechanically initiated samples, but only at high impact energies with nanopowder samples
- Mechanical initiated HEBM samples show slow reaction mode and ignition in shear bands, but no TE mode

Acknowledgements

- Dr. Paul Kotula for TEM images
- This work was supported by:
- Office of Naval Research
- DTRA
- Laboratory Directed Research and Development program at Sandia National Laboratories.
- Sandia National Laboratories is a multi-program laboratory managed and operated by Sandia Corporation, a wholly owned subsidiary of Lockheed Martin Corporation, for the U.S. Department of Energy's National Nuclear Security Administration under contract DE-AC04-94AL85000.

- Questions?